Electronic Supplementary Material (ESI)
This journal is © The Royal Society of Chemistry 2023

A translationally active ligand based on a [2]rotaxane molecular shuttle with a 2,2'-bipyridyl core

Ayan Dhara, Anton Dmitrienko, Rahaf N. Hussein, Ariel Sotomayor, Benjamin H. Wilson, and Stephen J. Loeb*

Department of Chemistry and Biochemistry
University of Windsor, Windsor, Ontario, N9B 3P4 Canada

Table of Contents

1. General Comments

All reagents were obtained from commercial suppliers and used as received unless stated otherwise. The building block **2** was synthesized according to the reported literature procedure.[S1,S2] Column chromatography was performed on silica gel (40-63 μm). Thin layer chromatography (TLC) was performed on pre-coated silica gel plates (250 μm thick, TLG-R10011B-323, Silicycle, Canada) and read under UV light.

Nuclear magnetic resonance (NMR) spectra (^{1}H, ^{13}C, ^{1}H-^{1}H COSY, 2D EXSY and ROESY) were recorded on a Bruker Avance III console equipped with an 11.7 T magnet, $\nu_o(^{1}H)$ = 500 MHz and $\nu_o(^{13}C)$ = 125.7 MHz, or on a Bruker Avance Ultra-shield console equipped with a 7.0 T magnet, $\nu_o(^{1}H)$ = 300 MHz and $\nu_o(^{13}C)$ = 75.4 MHz. Chemical shifts were quoted in ppm and referenced to corresponding residual solvent peaks. High-resolution electrospray ionization (ESI) mass spectrometry was performed on a Thermo Electron Corporation MAT 95XP-Trap mass spectrometer.

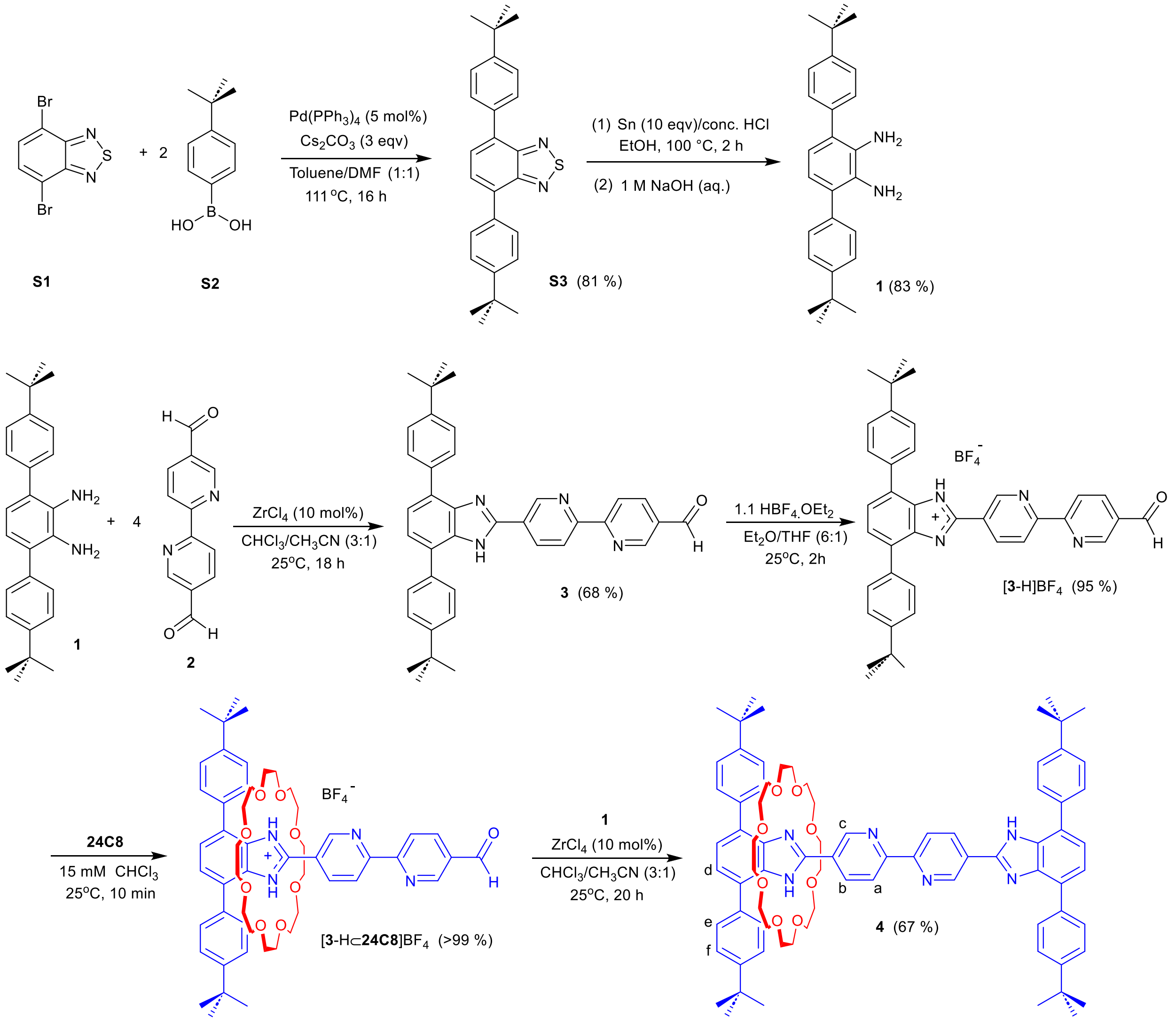

Scheme S1. Summary of the synthesis of [2]rotaxane ligand **4**.

2. Synthesis of 1

1 was synthesized using a modified literature procedure.[S3] **S3** (420 mg, 1.1 mmol, 1.0 equivalent) was suspended in ethanol (150 mL), and the suspension heated to 100 °C to dissolve **S3**. Concentrated HCl (10 mL) was added to the hot yellow solution. Afterwards, tin (1.3 g, 11.0 mmol, 10.0 equivalent) was added to the reaction mixture in three portions every 30 min. After 2h, the solution became colourless and was cooled to room temperature. The reaction was quenched with water (100 mL), and the product extracted with Et_2O (3×50 mL). The combined organic layers were further washed with water (3×50 mL). Finally, the organic extract was basified with aqueous 1M NaOH (200 mL), dried over anhydrous $MgSO_4$, and all solvents were evaporated under reduced pressure to give **1** (340 mg, 0.91 mmol, 83%) in 96% yield (see Figure S1) as a white solid. This material was used directly in the next step without any further purification. The ^1H NMR spectrum of **1** was consistent with the reported data.[S3]

^1H NMR (CD_2Cl_2, 300 MHz, 298 K): δ 7.50 (d, *J* = 8.4 Hz, 4H), 7.40 (d, *J* = 8.5 Hz, 4H), 6.72 (s, 2H), 3.64 (br s, 2H), 1.37 (s, 18H).

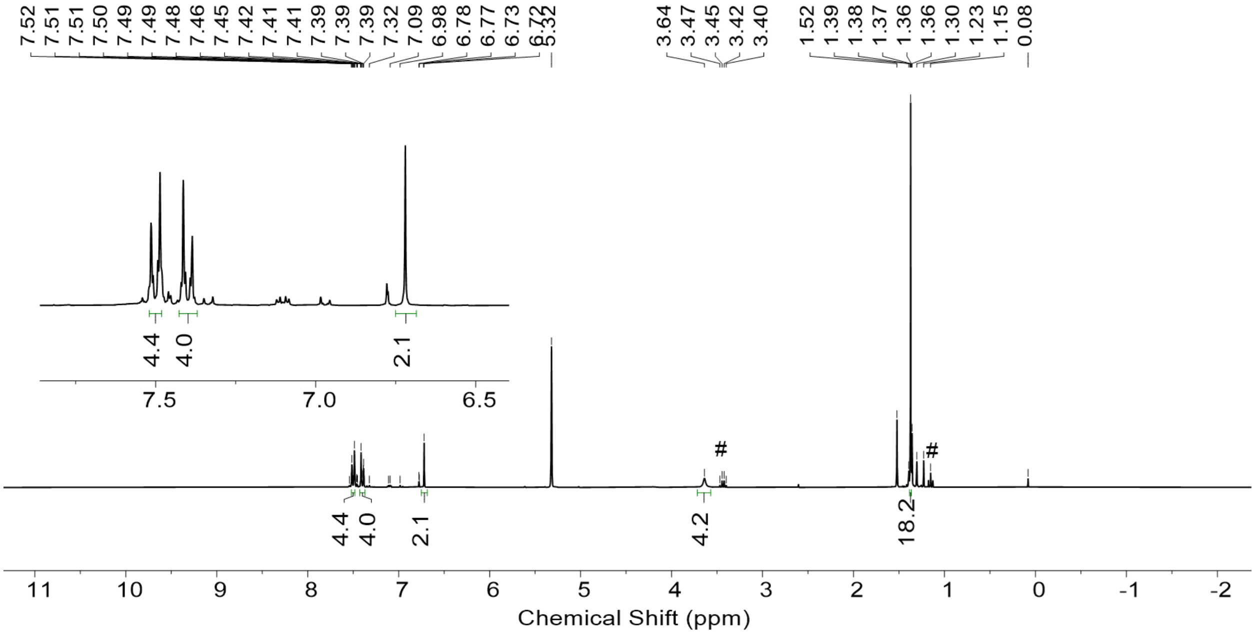

Figure S1. ^1H NMR spectrum of **1** (300 MHz, CD_2Cl_2, 298 K). # = Et_2O

3. Synthesis of 3

1 (158 mg, 0.424 mmol, 1.0 equivalent) and **2** (361 mg, 1.70 mmol, 4.0 equivalent) were dissolved in a mixture of chloroform (60 mL) and acetonitrile (20 mL). $ZrCl_4$ (10 mg, 0.0424 mmol, 0.1 equivalent) was added to the resulting yellow solution, and the mixture was stirred overnight at room temperature. After 18 h, Et_3N (2 mL) was added to the reaction mixture, and the solution stirred for five minutes. Afterwards, all solvents were evaporated resulting in a dark yellow precipitate. Dichloromethane (50 mL) was added to the crude solid, and the resulting suspension was filtered. The filtrate was evaporated and subjected to column chromatography (Eluent: EtOAc/$CHCl_3$ = 1:9) to obtain pure **3** (162 mg, 0.287 mmol, 68 %) as a light-yellow solid which was used directly in the next step. Higher purity product for full characterization was obtained by heating a suspension of the solid precipitate at 80 °C in acetonitrile for 0.5 h, filtering the solution and concentrating the filtrate.

^{1}H NMR (DMSO-d$_6$, 500 MHz, 298 K): δ 12.98 (s, 1H), 10.20 (s, 1H), 9.64 – 9.63 (m, 1H), 9.23 (d, *J* = 2.2 Hz, 1H), 8.92 – 8.81 (m, 1H), 8.66 (dd, *J* = 13.4, 8.3 Hz, 2H), 8.44 (dd, *J* = 8.2, 2.1 Hz, 1H), 8.14 (d, *J* = 8.1 Hz, 2H), 7.72 (d, *J* = 7.8 Hz, 2H), 7.64 – 7.51 (m, 5H), 7.36 (d, *J* = 7.7 Hz, 1H), 1.39 (d, *J* = 6.7 Hz, 18H).

^{13}C NMR (DMSO-d$_6$, 125.7 MHz, 298 K): δ 192.08, 158.77, 154.43, 151.57, 150.02, 149.64, 149.47, 148.49, 142.02, 137.38, 135.91, 135.17, 134.94, 133.60, 131.29, 129.84, 128.60, 128.14, 127.06, 125.75, 125.14, 125.04, 123.73, 121.40, 121.08, 34.43, 34.35, 31.20.

HRMS (ESI) *m/z*: [**3**+H]$^+$ Calcd for $C_{38}H_{37}N_4O^+$ 565.2962; Found 565.2965

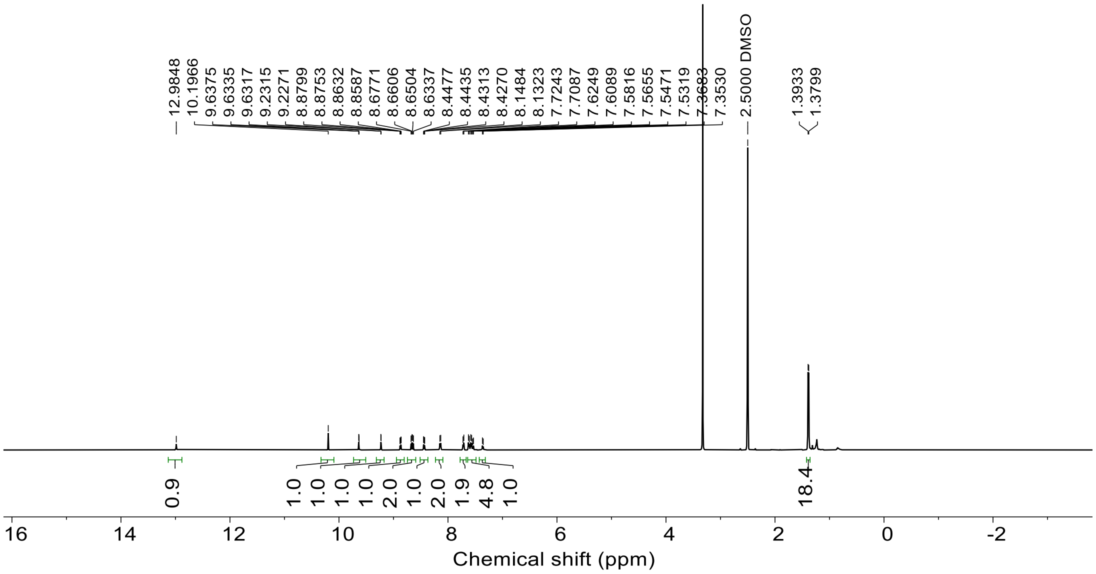

Figure S2. ^{1}H NMR spectrum of **3** (500 MHz, DMSO-d$_6$, 298 K).

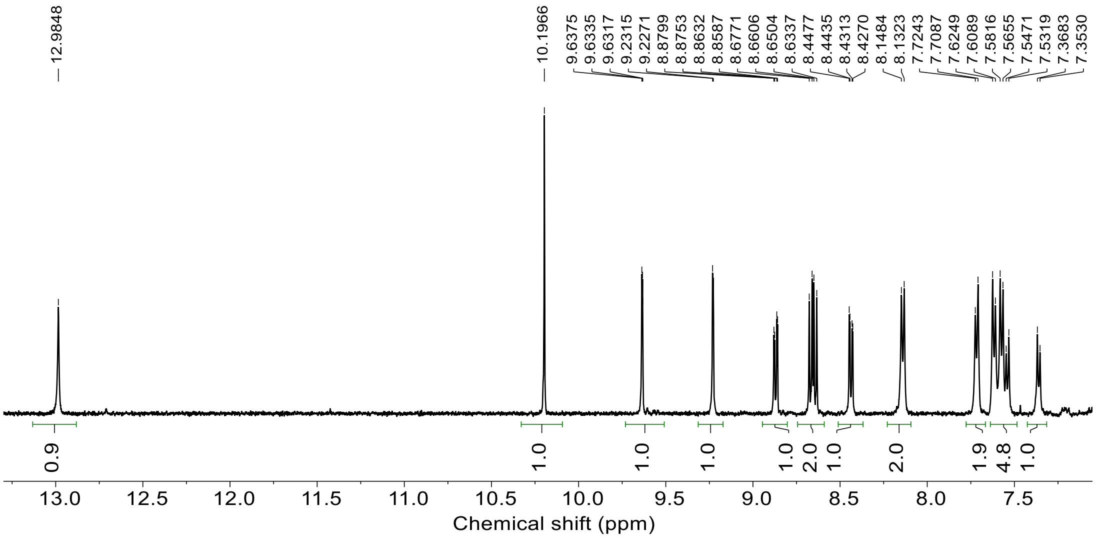

Figure S3. Aromatic region of the ^{1}H NMR spectrum of **3** (500 MHz, DMSO-d$_6$, 298 K).

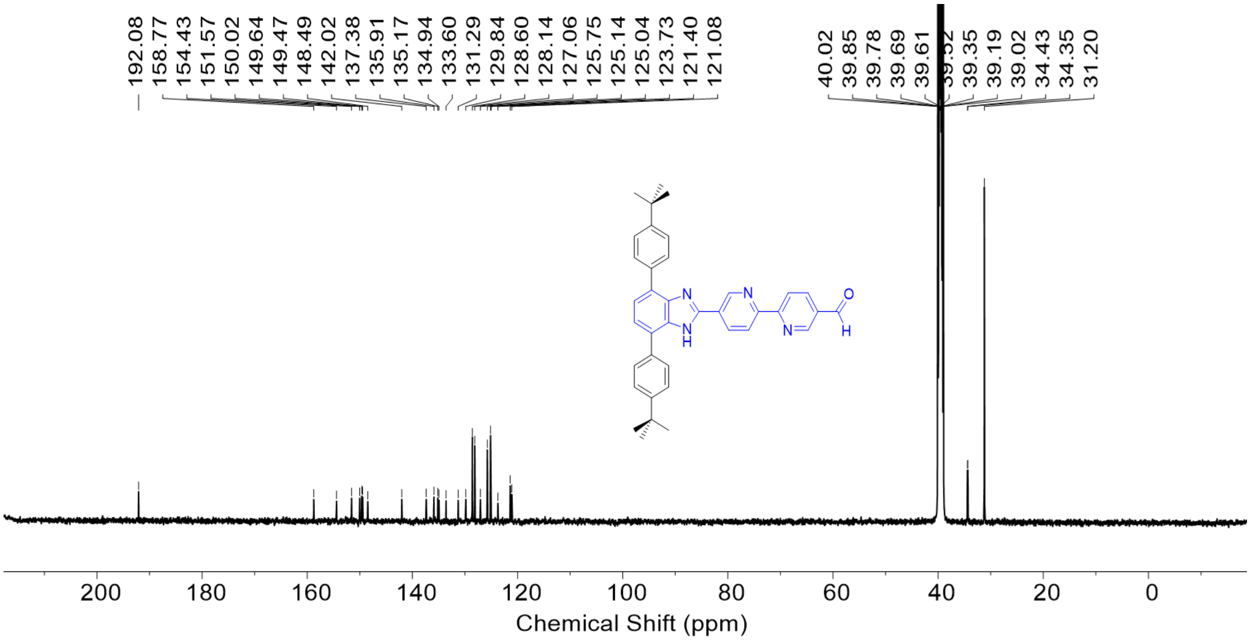

Figure S4. ^{13}C NMR spectrum of **3** (125.7 MHz, DMSO-d$_6$, 298 K).

4. Synthesis of [3-H]BF$_4$

3 (162 mg, 0.287 mmol, 1.0 equivalent) was dissolved in a mixture of Et$_2$O (30 mL) and THF (5 mL). HBF$_4$·Et$_2$O (43 µL, 51.0 mg, 0.316 mmol, 1.1 equivalent) was added to the yellow solution. The solution immediately produced a red suspension which was stirred for 2 h at room temperature. Afterwards [**3**-H]BF$_4$ was separated, washed with Et$_2$O (3×20 mL), and dried in air as to yield a red precipitate (178 mg, 0.273 mmol, 95 %).

^{1}H NMR (CD$_3$CN, 500 MHz, 298 K): δ 10.20 (s, 1H), 9.31 (dd, *J* = 2.4, 0.8 Hz, 1H), 9.21 (dd, *J* = 2.1, 0.8 Hz, 1H), 8.80 (dd, *J* = 8.4, 0.8 Hz, 1H), 8.71 (d, *J* = 8.2 Hz, 1H), 8.61 (dd, *J* = 8.4, 2.4 Hz, 1H), 8.44 (dd, *J* = 8.2, 2.1 Hz, 1H), 7.77 – 7.66 (m, 10H), 1.42 (s, 18H).

^{13}C NMR (CD$_3$CN, 125.7 MHz, 298 K): δ 192.24, 153.18, 152.18, 149.64, 139.86, 138.93, 133.68, 133.31, 129.51, 128.77, 127.90, 127.37, 118.31, 68.30, 35.48, 31.59, 26.25, 1.49, 1.32, 1.16.

HRMS (ESI) *m/z*: [**3**-H]$^+$ Calcd for $C_{38}H_{37}N_4O^+$ 565.2962; Found 565.2965

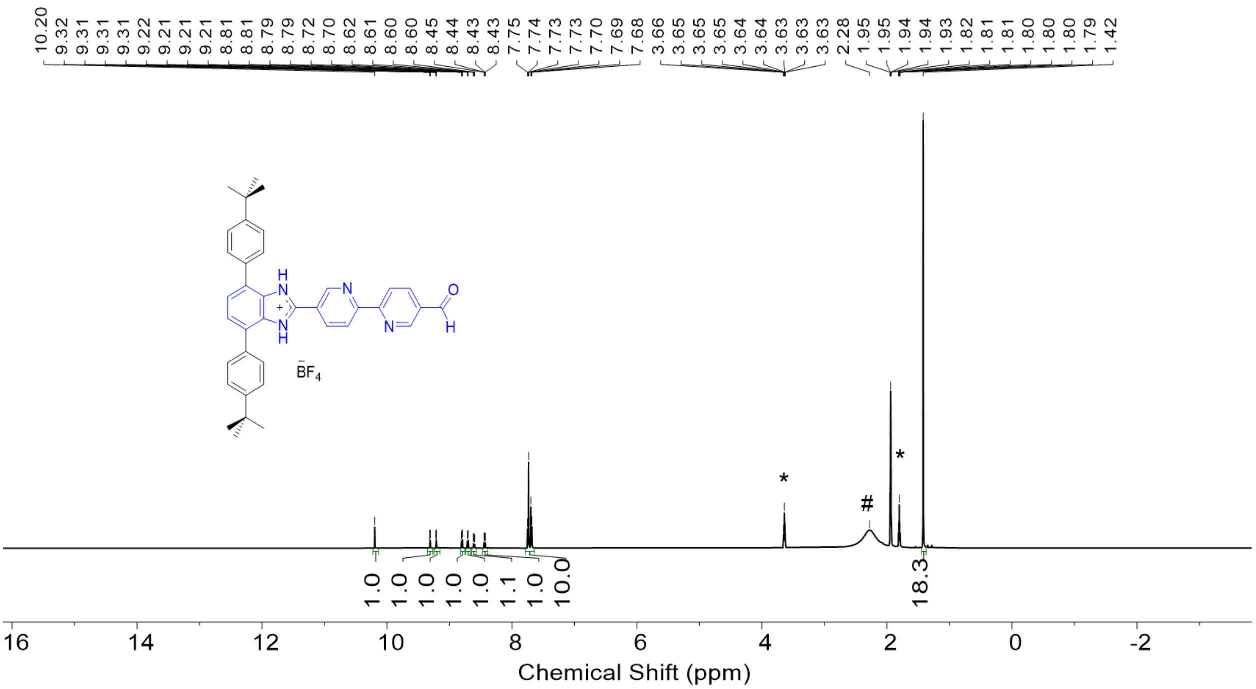

Figure S5. ^1H NMR spectrum of [**3**-H]BF_4 (500 MHz, CD_3CN, 298 K). * = THF, # = water.

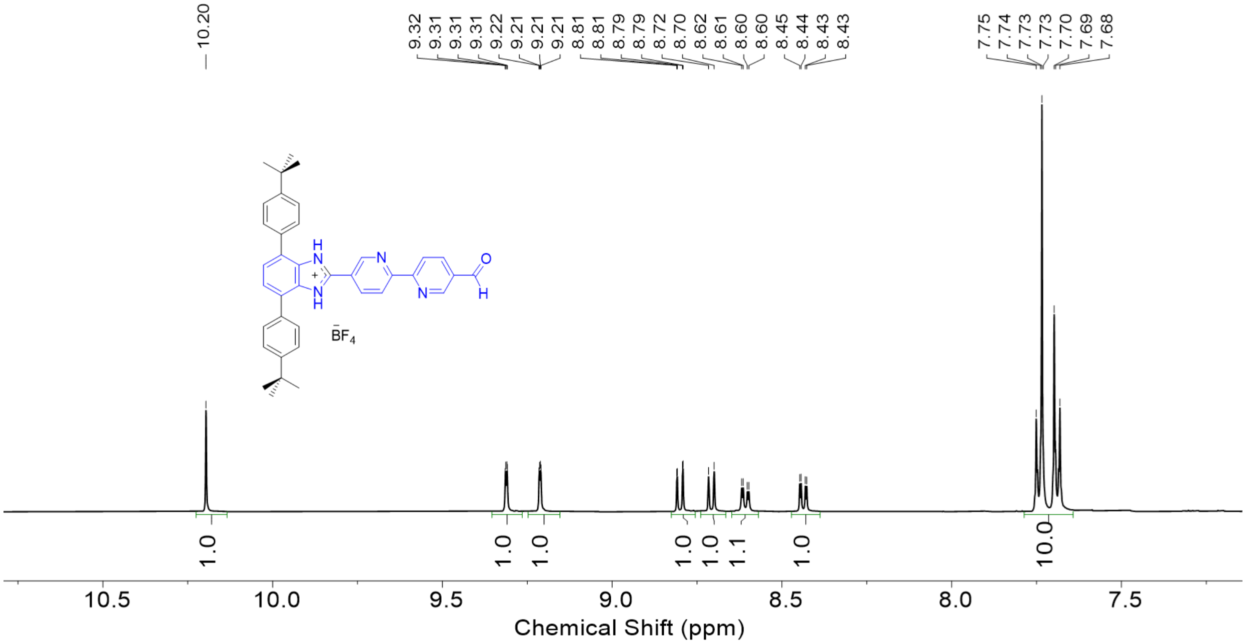

Figure S6. Aromatic region of the ^1H NMR spectrum of [**3**-H]BF_4 (500 MHz, CD_3CN, 298 K).

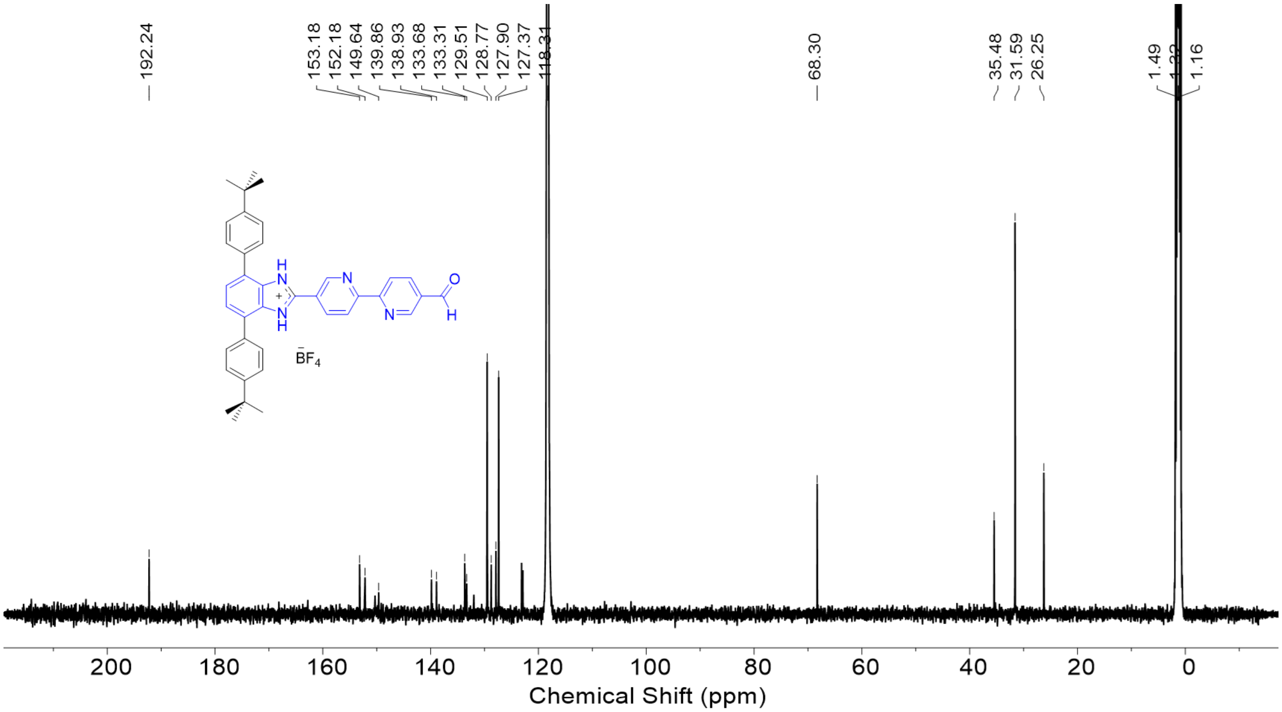

Figure S7. ^{13}C NMR spectrum of [**3**-H]BF_4 (125.7 MHz, CD_3CN, 298 K).

5. Synthesis of 4

[**3**-H]BF_4 (185 mg, 0.284 mmol, 1.0 equivalent) was suspended in chloroform (20 mL), and **24C8** (150 mg, 0.426 mmol, 1.5 equivalent) added to the red suspension. The red suspension immediately turned into a light-yellow solution. The solution was stirred for 10 min. Afterwards, **1** (106 mg, 0.284 mmol, 1.0 equivalent) was added to produce a relatively dark yellow solution. $ZrCl_4$ (6.6 mg, 0.0284 mmol, 0.1 equivalent) was then added to the solution, and the reaction mixture was stirred overnight at room temperature. After 18 h, Et_3N (2 mL) was added to the reaction mixture. The colour of the solution changed from dark orange to yellow. After 10 min of stirring, all solvents were evaporated to yield crude product, which was subjected to column chromatography (Eluent: MeOH/CH_2Cl_2 = 1:10). The solvents of the product fraction were evaporated, and the solid residue was redissolved in a mixture of acetonitrile (5 mL) and dichloromethane (15 mL), followed by addition of Et_3N (2 mL) to the solution. All solvents were removed, and the resulting precipitate was washed with Et_2O (3 × 20 mL). The final precipitate was dried under vacuum to yield **4** as a yellowish white solid (240 mg, 0.189 mmol, 67 %).

^{1}H NMR (CD_2Cl_2, 500 MHz, 298 K): Only broadened and averaged peaks were observed at room temperature due to shuttling of the **24C8** macrocycle along the rotaxane axle which was fast on the NMR timescale. See Figure S9 for the variable temperature ^{1}H NMR spectra of **4** and Figure S10 for the ^{1}H NMR spectrum of [**4**-H]BF_4 in which the **24C8** macrocycle is locked in position producing a single set of resonances for this static structure.

HRMS (ESI) *m/z*: [**4**+H]$^+$ Calcd for $C_{80}H_{97}N_6O_8^+$ 1269.7362; Found 1269.7378

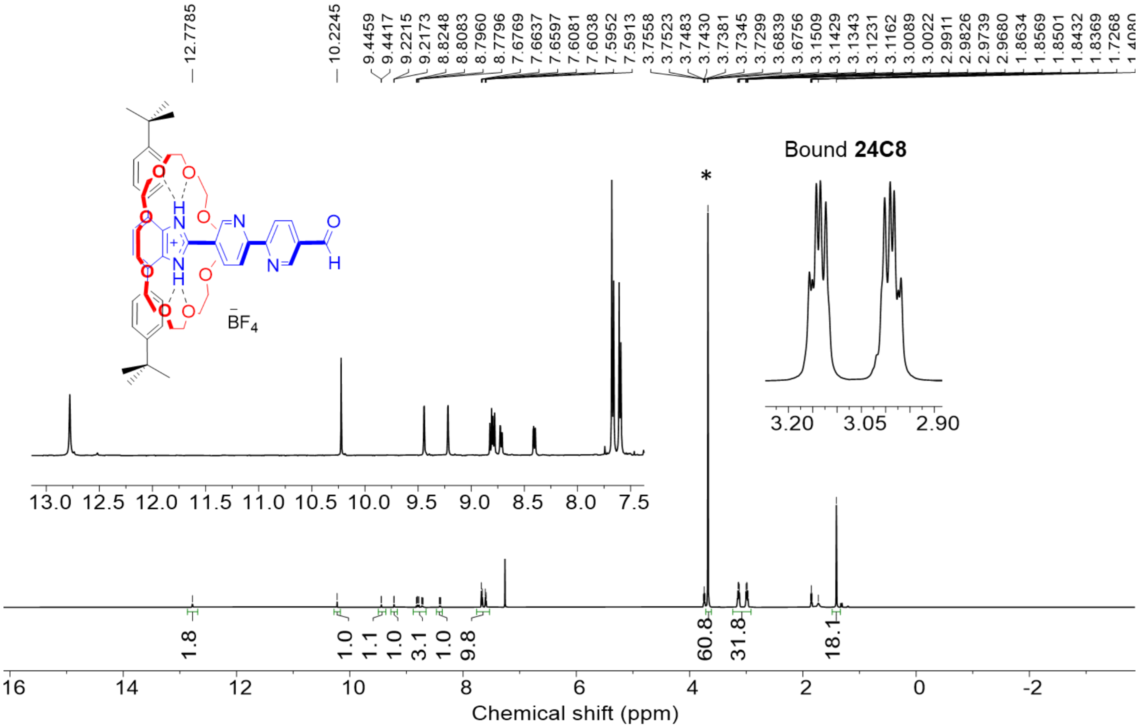

Figure S8. ^{1}H NMR spectrum of [**3**-H$\subset$**24C8**]BF$_4$ (500 MHz, CDCl$_3$, 298 K). * = unbound **24C8**

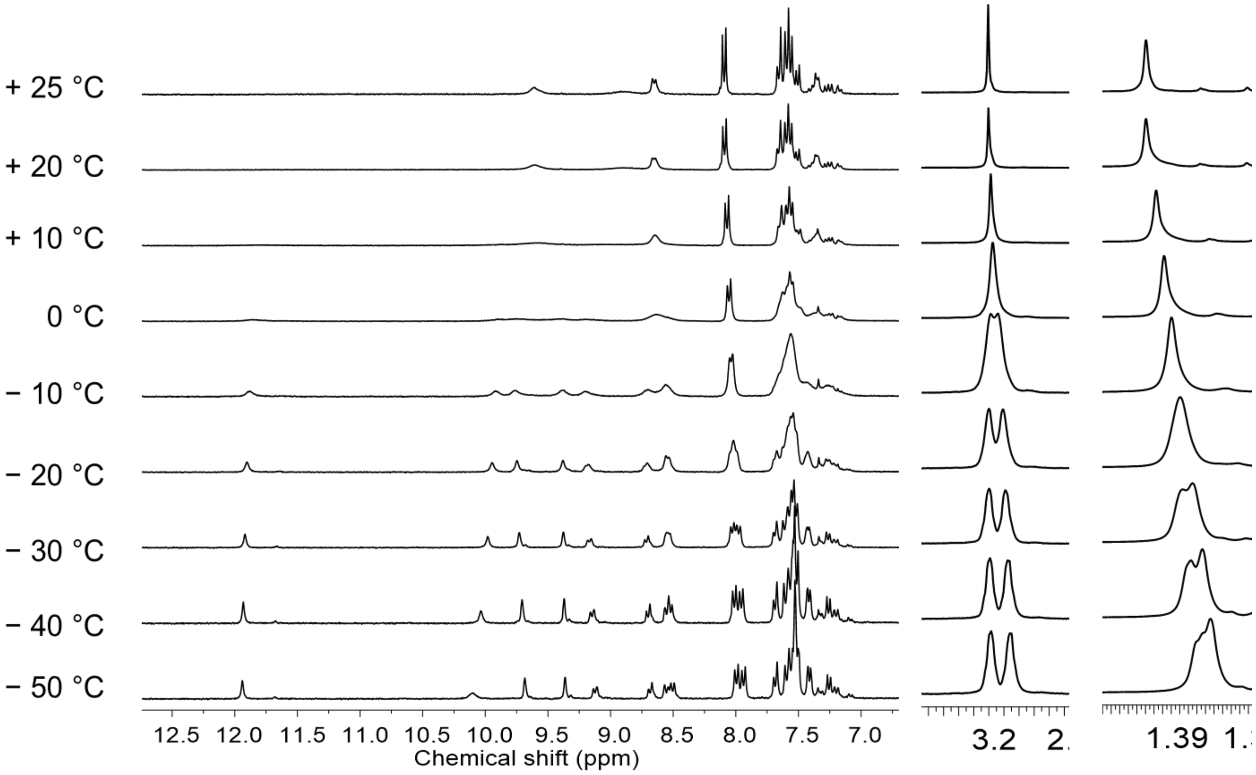

Figure S9. ^{1}H NMR spectra of **4** at various temperatures (300 MHz, CD$_2$Cl$_2$).

The shuttling rates (k) at temperatures – 50 °C, – 40 °C, – 30 °C, – 20 °C and – 10 °C were determined using line shape analysis by fitting simulated and measured 1D NMR spectra. This was accomplished utilising the DNMR (Dynamic NMR) module in the Bruker Topspin suite of NMR programs. A best fit plot of ln(k/T) vs. 1/T yielded a shuttling rate of 61.2 s^{-1} at 25 °C. The Eyring equation was used to calculate $\Delta G^{\ddagger}$ at 25 °C:

$$\Delta G^{\ddagger} = -RT\ln\left(\frac{kh}{k_{B}T}\right) = 15.1\ \text{kcal/mol}$$

where R is the ideal gas constant, h is Plank's constant, and k_B is Boltzmann's constant.

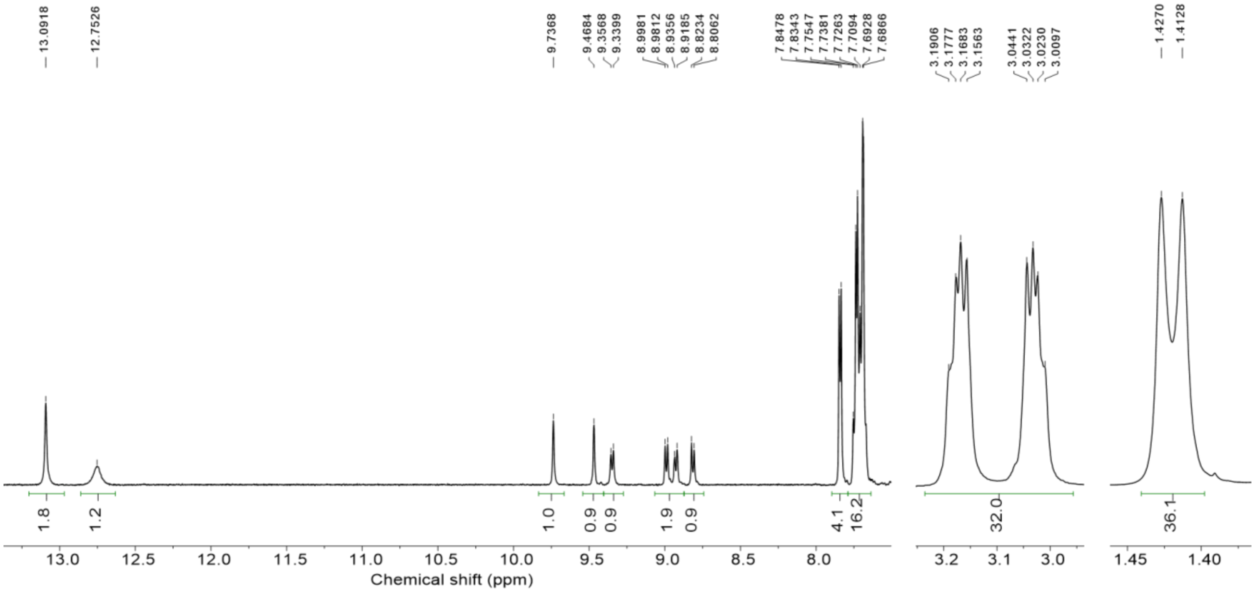

Figure S10. ^{1}H NMR spectrum of [**4**-H]BF_4 (500 MHz, CD_3CN, 298 K).

6. Synthesis of [$PtCl_2$(4)]

4 (25 mg, 0.020 mmol, 1.0 equivalent) and $PtCl_2(DMSO)_2$ (13 mg, 0.030, 1.5 equivalents) were dissolved in a mixture of acetonitrile (20 mL) and chloroform (10 mL). The solution was heated to 100 °C for 16 h. Afterwards, the solution was cooled to room temperature and all solvents were removed to yield a yellow precipitate. The crude precipitate was suspended in a basic solution of acetonitrile (0.1 mL Et_3N in 10 mL acetonitrile) and left at room temperature overnight. The yellow precipitate was then separated and further washed three times with a basic solution of acetonitrile (0.05 mL Et_3N in 5 mL acetonitrile). The final product [$PtCl_2$(**4**)] (17 mg, 0.011 mmol, 55 %) was dried in air.

^{1}H NMR (CD_2Cl_2, 500 MHz, 298 K): δ 12.95 (s, 1H), 10.58 (s, 1H), 10.36 (d, J = 1.9 Hz, 1H), 10.24 (d, J = 2.0 Hz, 1H), 9.85 (dd, J = 8.5, 1.9 Hz, 1H), 9.07 (dd, J = 8.5, 2.0 Hz, 1H), 8.21 (dd, J = 15.4, 8.6 Hz, 2H), 8.12 – 8.06 (m, 4H), 7.69 – 7.45 (m, 15H), 7.31 (d, J = 7.6 Hz, 1H), 3.24 (br s, 32H), 1.47 – 1.36 (m, 36H).

^{13}C NMR (CD_2Cl_2, 125.7 MHz, 298 K): The solubility of the complex was not sufficient to collect a suitable ^{13}C NMR spectrum (see Figure S13).

HRMS (ESI) *m/z*: [[$PtCl_2$(**4**)] + H]$^+$ Calcd for $C_{80}H_{97}Cl_2N_6O_8^+$ 1535.6400; Found 1535.6393

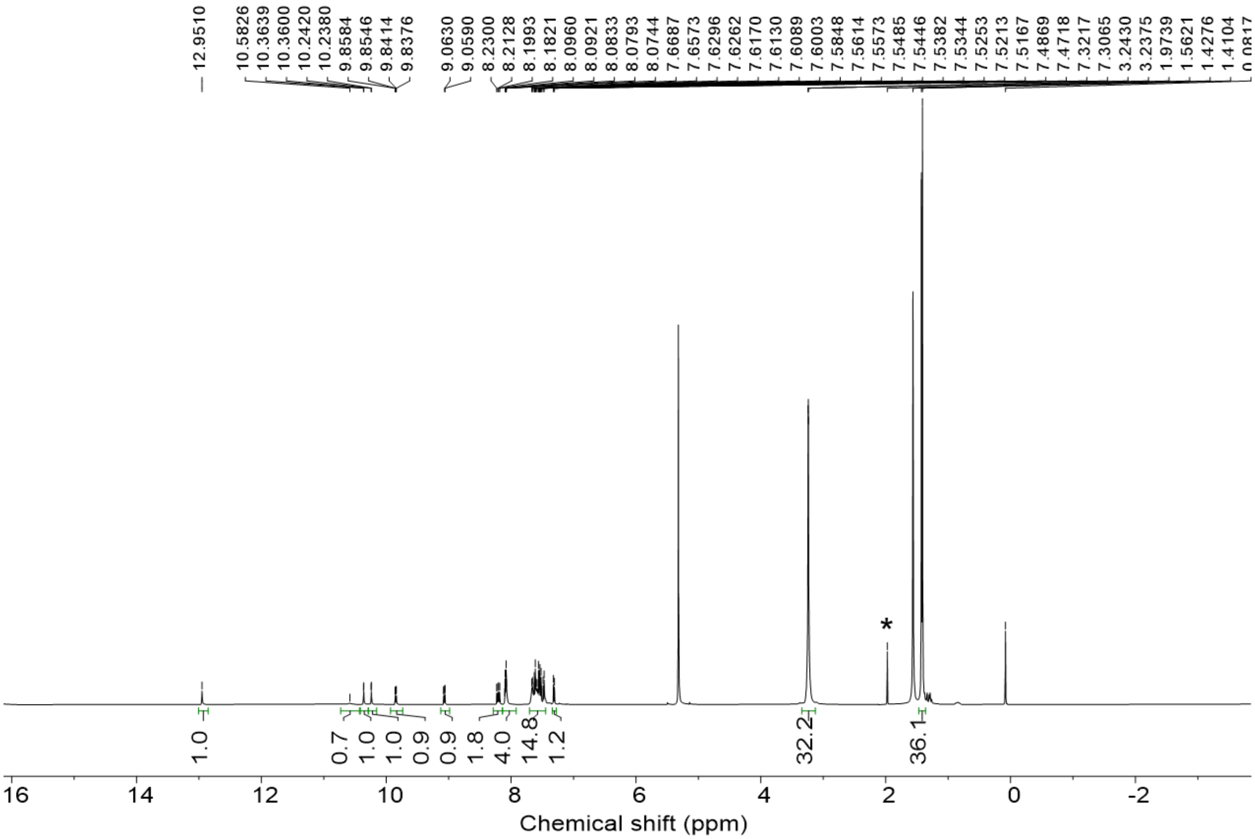

Figure S11. ^{1}H NMR spectrum of [PtCl$_2$(**4**)] (500 MHz, CD$_2$Cl$_2$, 298 K). * = acetonitrile

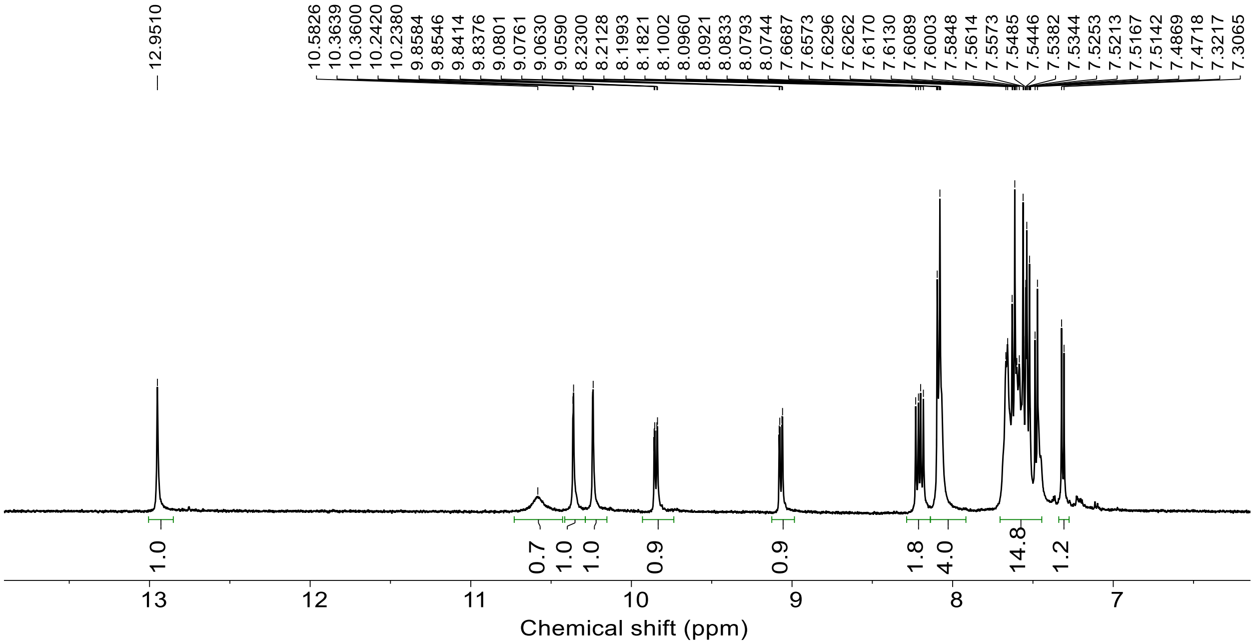

Figure S12. The aromatic region of ^{1}H NMR spectrum of [PtCl$_2$(**4**)] (500 MHz, CD$_2$Cl$_2$, 298 K).

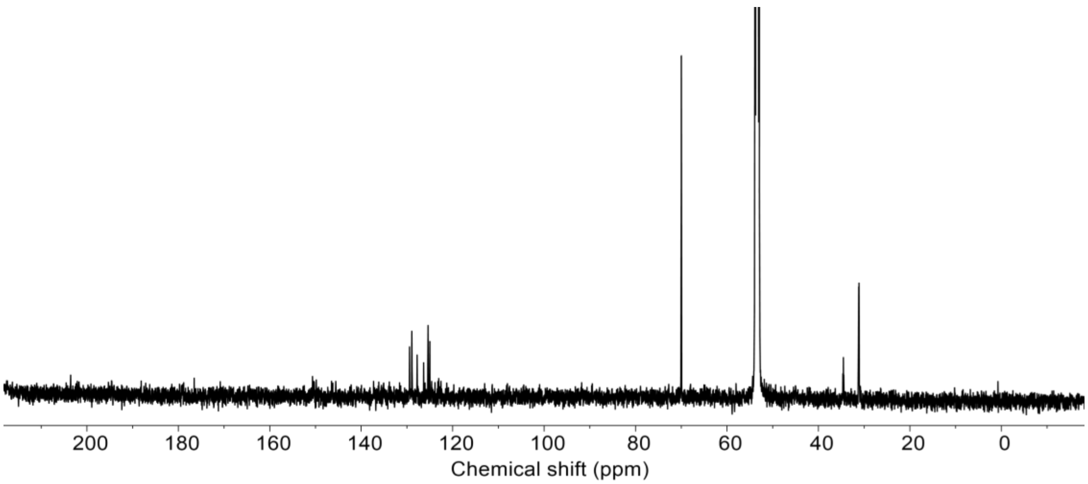

Figure S13. ^{13}C NMR spectrum of [PtCl$_2$(**4**)] (125.7 MHz, CD$_2$Cl$_2$, 298 K).

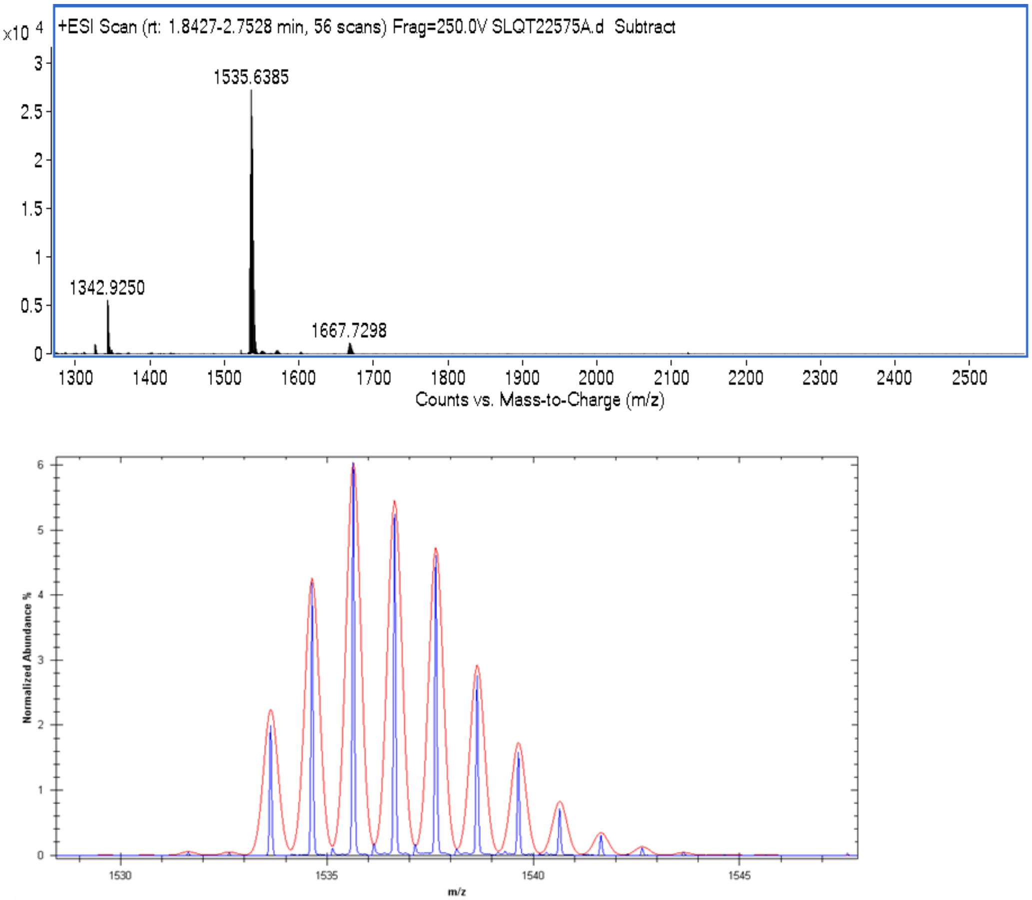

Figure S14. ESI-MS (+ve) of [PtCl$_2$(**4**)] top. Observed (blue) and calculated (red) pattern for the ion [[PtCl$_2$(**4**)] + H]$^+$.

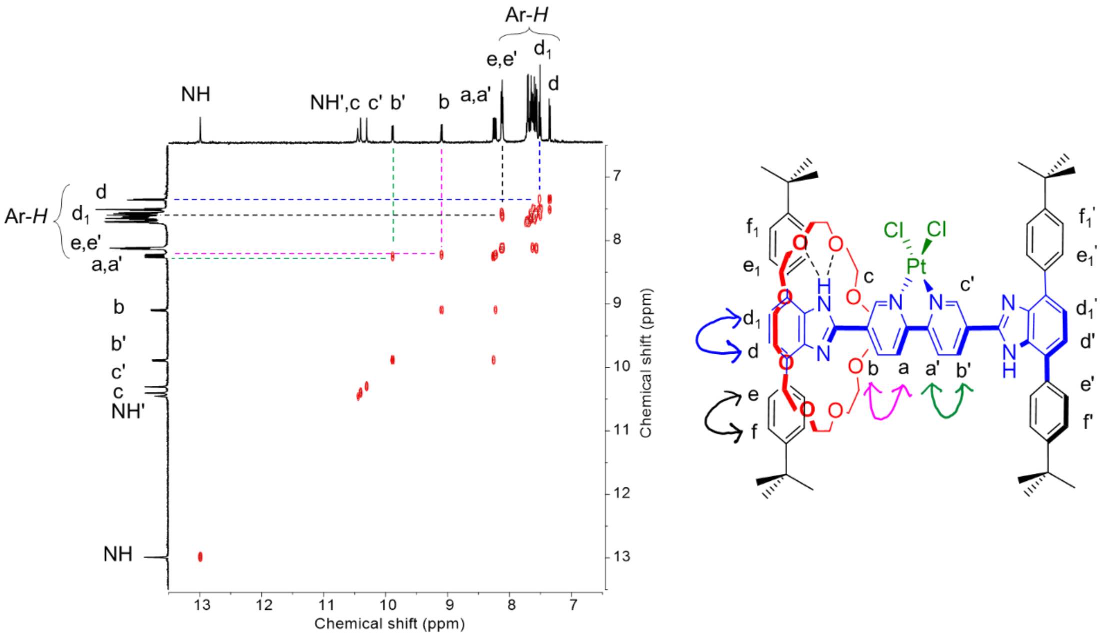

Figure S15. ^{1}H-^{1}H COSY NMR spectrum of [PtCl$_2$(**4**)] (500 MHz, CD$_2$Cl$_2$, 298 K).

7. Addition of NaBArF to [PtCl$_2$(4)]

To a solution of [PtCl$_2$(**4**)] (4.9 mg, 0.0032 mmol, 1 equivalent) in CD$_2$Cl$_2$ (0.6 mL) was added NaBArF (2.8 mg, 0.0032 mmol, 1 equivalent) at room temperature and NMR data was collected.

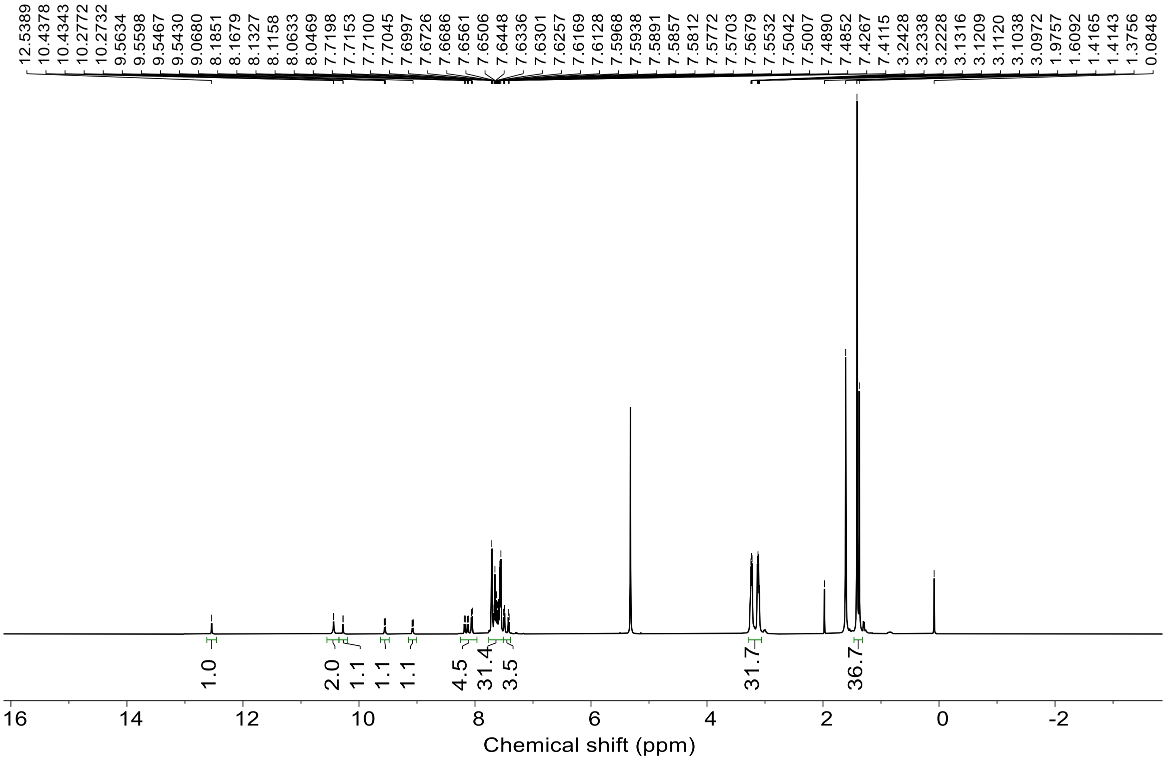

Figure S16. ^{1}H NMR spectrum of [PtCl(**4**)][BArF] (500 MHz, CD$_2$Cl$_2$, 298 K).

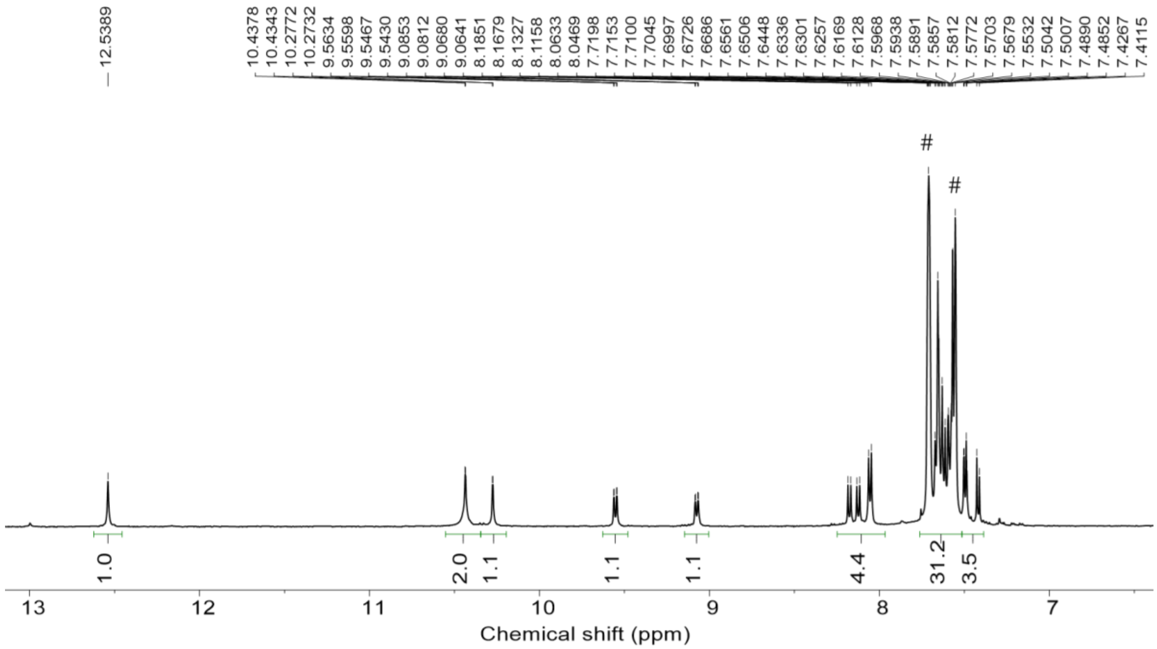

Figure S17. Aromatic region of the ^{1}H NMR spectrum of [PtCl(**4**)][BArF] (500 MHz, CD_2Cl_2, 298 K). # = ^{1}H NMR peaks corresponding to BArF anions.

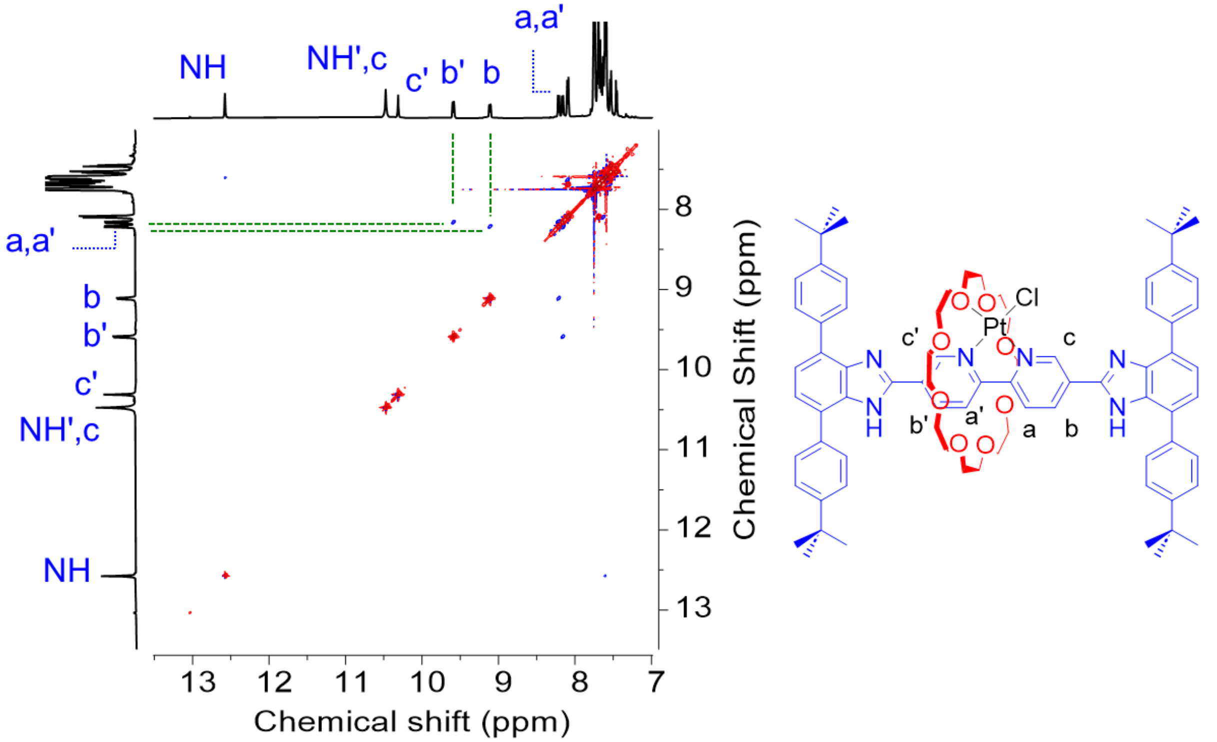

Figure S18. ^{1}H-^{1}H ROESY NMR spectrum of [PtCl(**4**)][BArF] (500 MHz, CD_2Cl_2, 298 K) showing cross-peaks between protons H_a and H_b.

8. Addition of Excess NaBArF to [PtCl$_2$(4)]

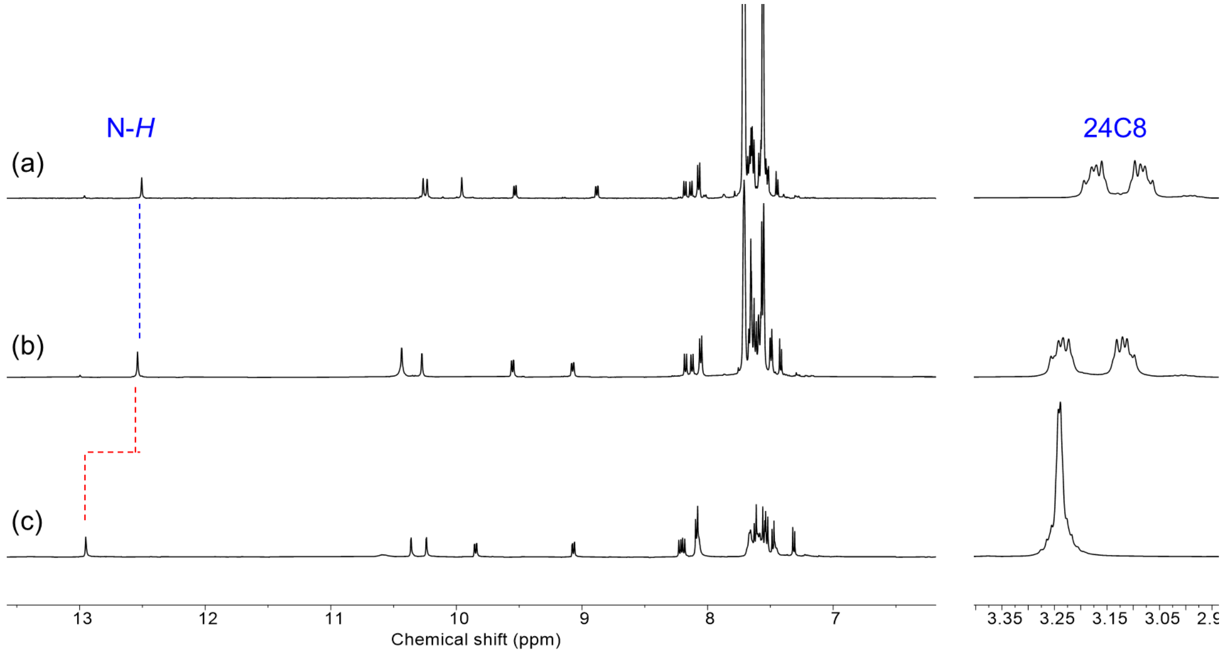

Figure S19. A comparison of the key regions of the ^{1}H NMR spectra of (a) [PtCl$_2$(**4**)] and [PtCl(**4**)][BArF] after the addition of (b) one equivalent and (c) four equivalents of NaBArF (500 MHz, CD$_2$Cl$_2$, 298 K). Note that the addition of four equivalents of NaBArF did not result in removal of the second the chloride ligand. In particular, no further change in chemical shift of the N-H or NMR signature for the crown ether **24C8** were observed, when more equivalents of NaBArF were added to [PtCl(**4**)][BArF]

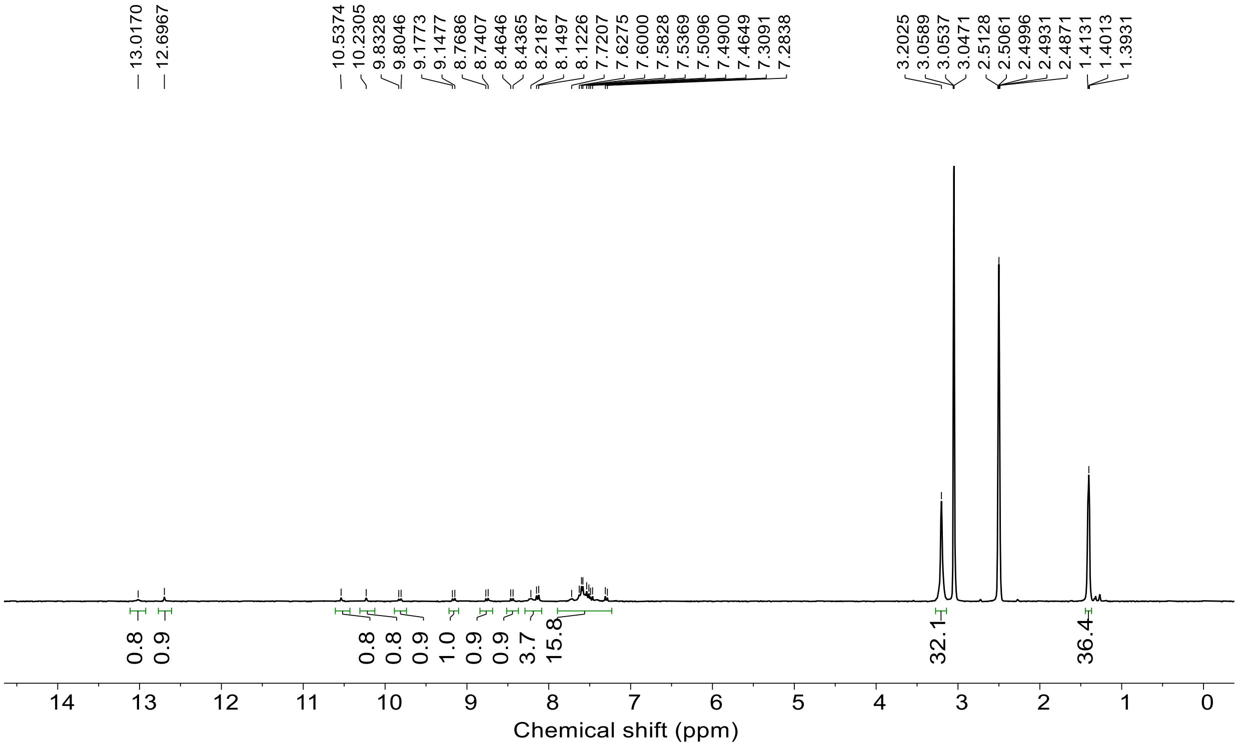

Figure S20. ^{1}H NMR spectrum of [PtCl$_2$(**4**)], (500 MHz, DMSO-d_6, 353 K). # = DMSO, * = H_2O

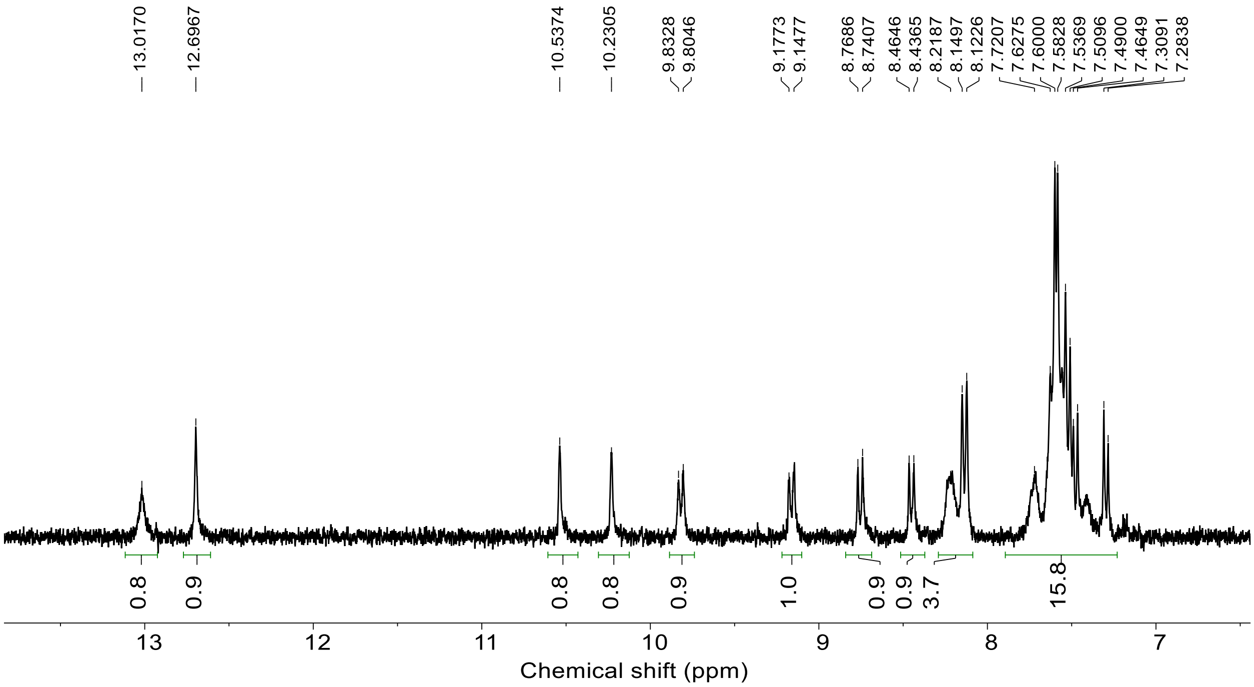

Figure S21. Aromatic region of the ^{1}H NMR spectrum of [$PtCl_2$(**4**)], (300 MHz, DMSO-d_6, 353 K).

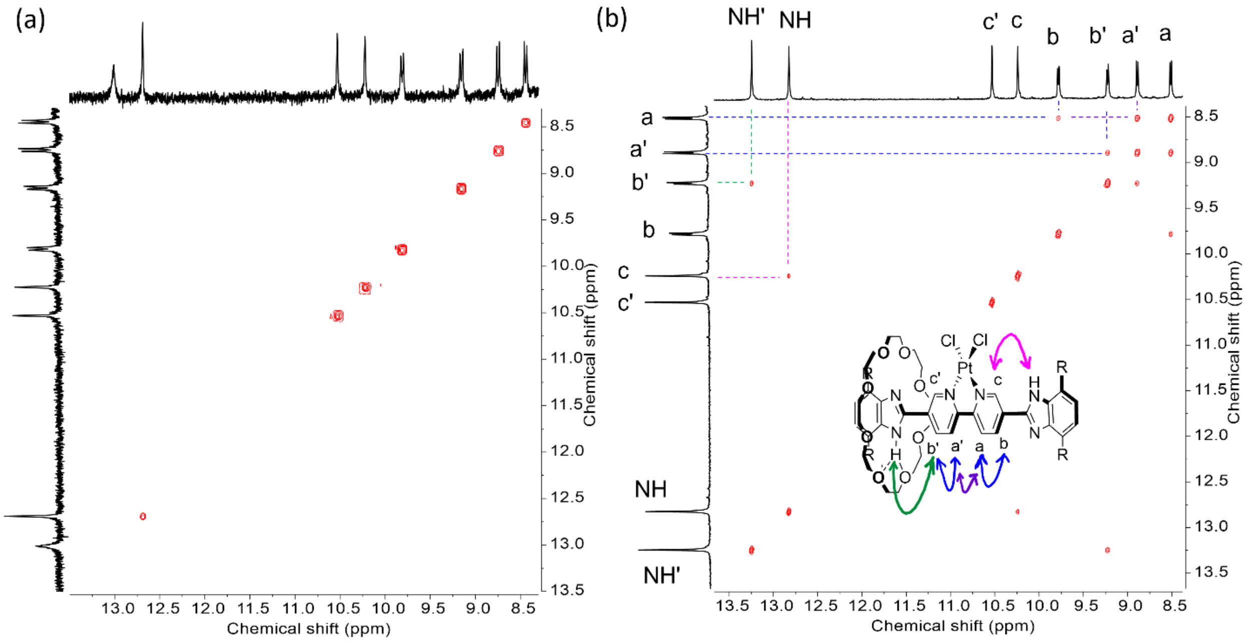

Figure S22. 1H-1H NOESY (EXSY) NMR of [PtCl2(**4**)]: (a) 300 MHz, DMSO-d_6, 353 K, mixing time = 800 ms. (b) 500 MHz, DMSO-d_6, 298 K, mixing time = 800 ms. No exchange peak between the N-H protons of the two benzimidazole groups was observed at either room temperature or high temperatures. The measurement at room temperature (298 K) allowed collection of an EXSY spectrum with more scans, which revealed cross-peaks used for peak assignments.

9. Synthesis of Zn(II) complexes of 4 in acetonitrile

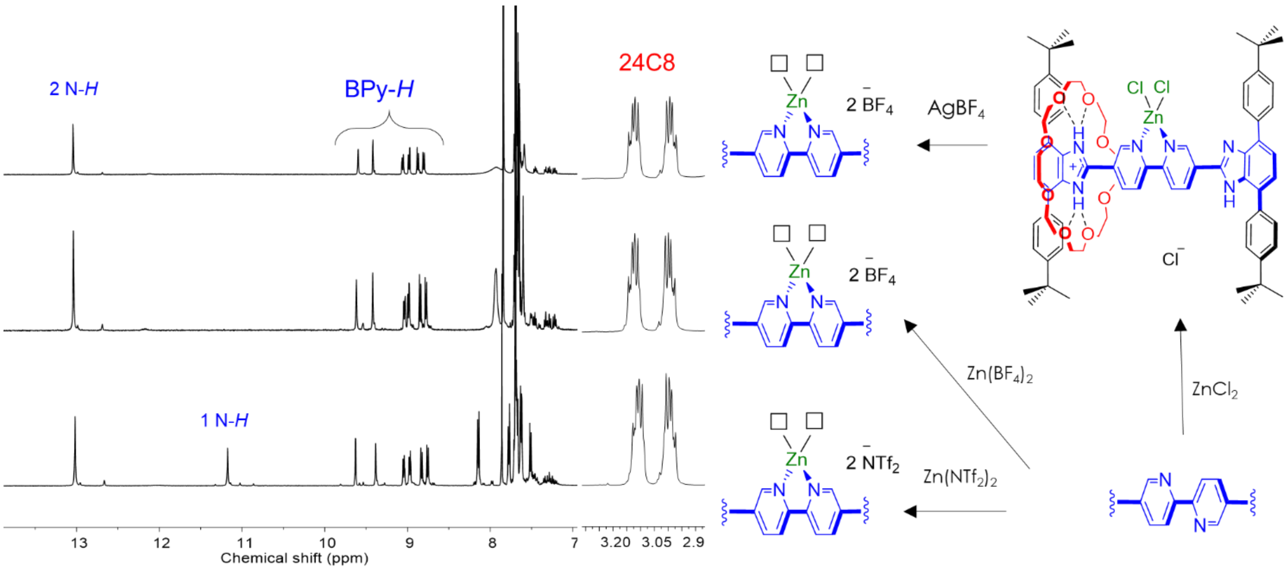

Figure S23. ^{1}H NMR spectra (500 MHz, CD_3CN, 298 K) showing the formation of Zn(II) complexes of **4** with different anions. In each case, a mono-protonated zinc complex of general formula [Zn(**4**-H)(solvent)$_2$]$^{3+}$ was formed in which one of the benzimidazole groups of the ligand was protonated while the other remained neutral (see diagram). The only difference among the spectra of these complexes was the observance of the NH resonance of the neutral benzimidazole group when the anion was triflimide. The same proton for the other zinc complexes was likely unobserved due to exchange with water present in the solvent used. All other features are identical and consistent with a static structure in which the crown ether is positioned at the charged benzimidazolium recognition site and no shuttling occurs.

It is very likely that generation of these monoprotonated species is due to activation of residual water in the presence of Lewis acidic Zn(II) ions in combination with the enhanced basicity of a rotaxane containing a basic nitrogen site on an axle in close proximity to an interlocked crown ether wheel.

10. ^{1}H NMR of 4 in DMF

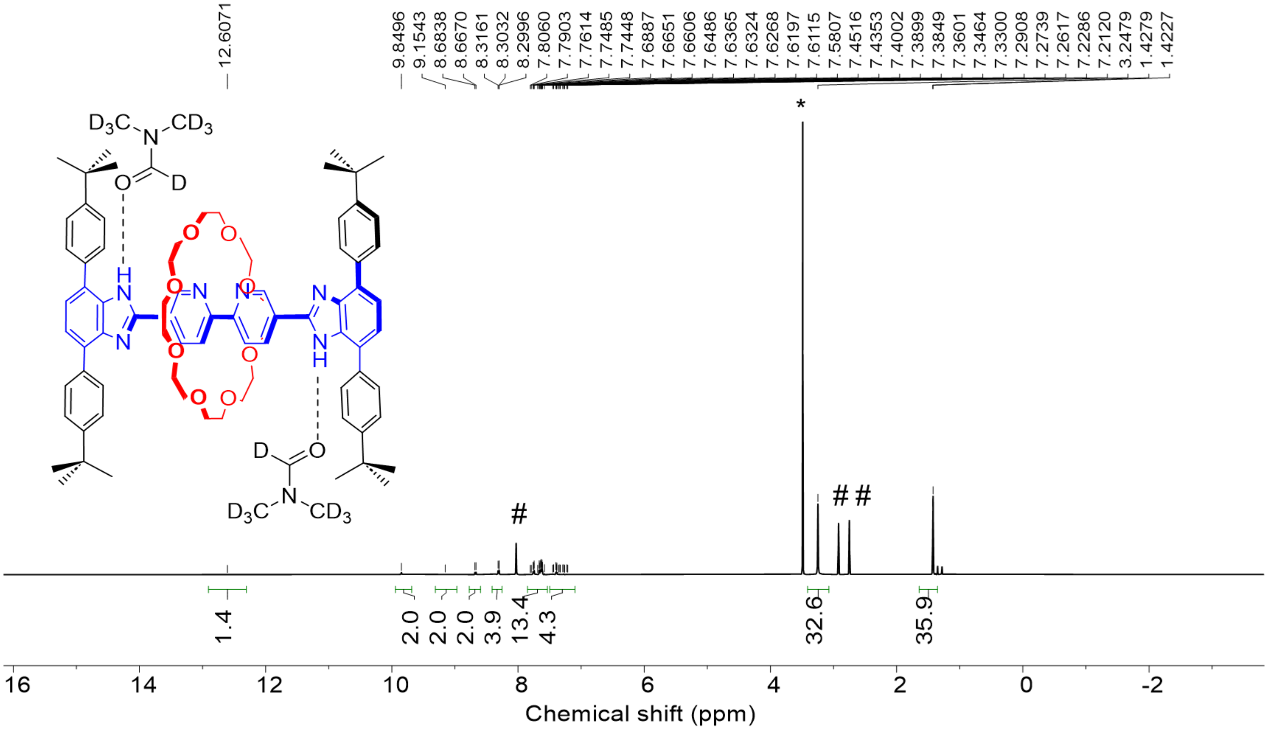

Figure S24. ^{1}H NMR spectrum of **4** (500 MHz, DMF-d_7, 298 K). # = residual DMF, * = water

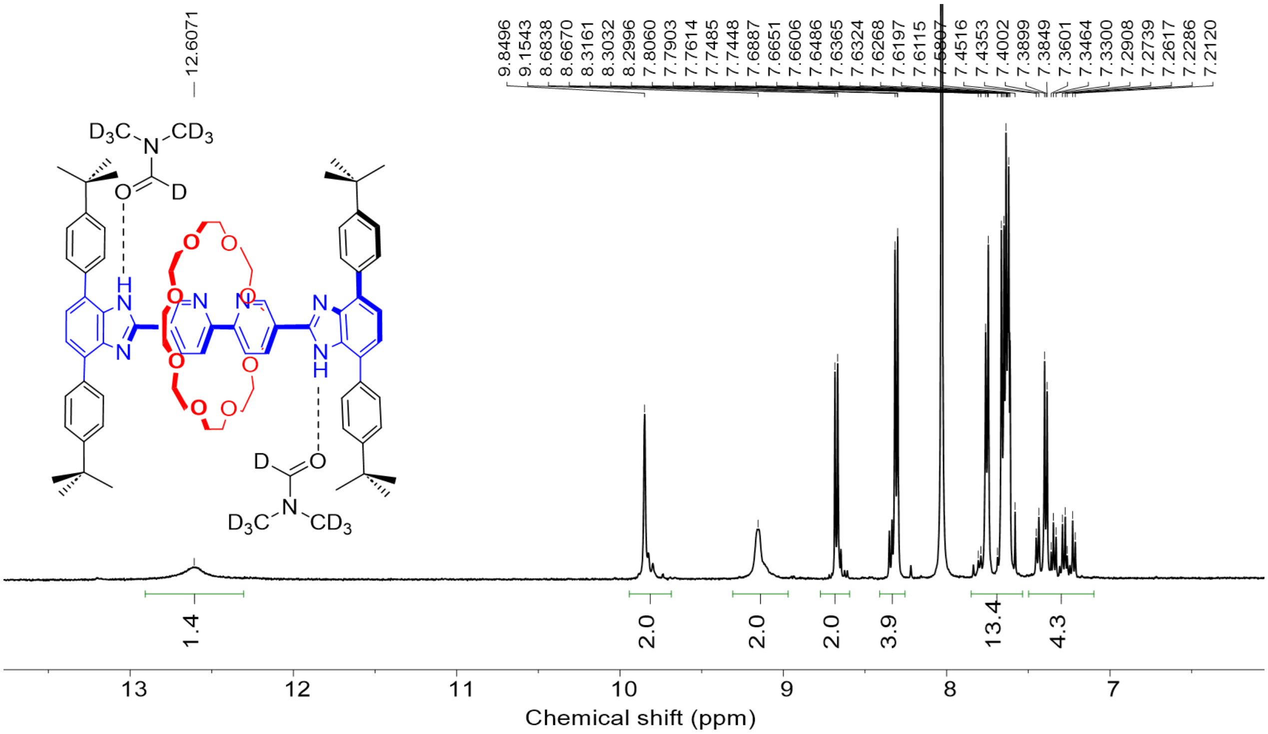

Figure S25. The aromatic region of ^{1}H NMR of **4** (500 MHz, DMF-d_7, 298 K).

11. Synthesis of [Zn(DMF)$_4$(4)][NTf$_2$]$_2$ in DMF

4 (3.6 mg, 0.0028 mmol, 1 equivalent) and Zn(NTf$_2$)$_2$ (1.8 mg, 0.0028 mmol, 1 equivalent) were dissolved in DMF-*d*$_7$ at room temperature to obtain a yellow solution. A ^{1}H NMR spectrum was recorded.

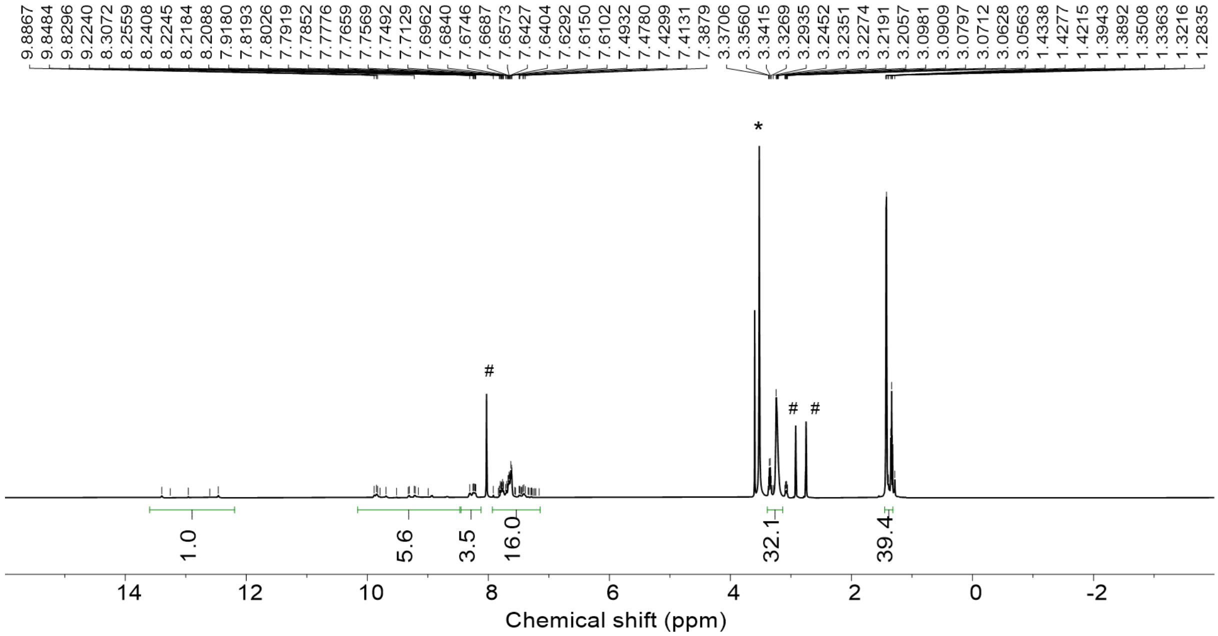

Figure S26. ^{1}H NMR spectrum of a 1:1 solution **4** and Zn(NTf$_2$)$_2$ (500 MHz, DMF-*d*$_7$, 298 K). # = residual DMF, * = water.

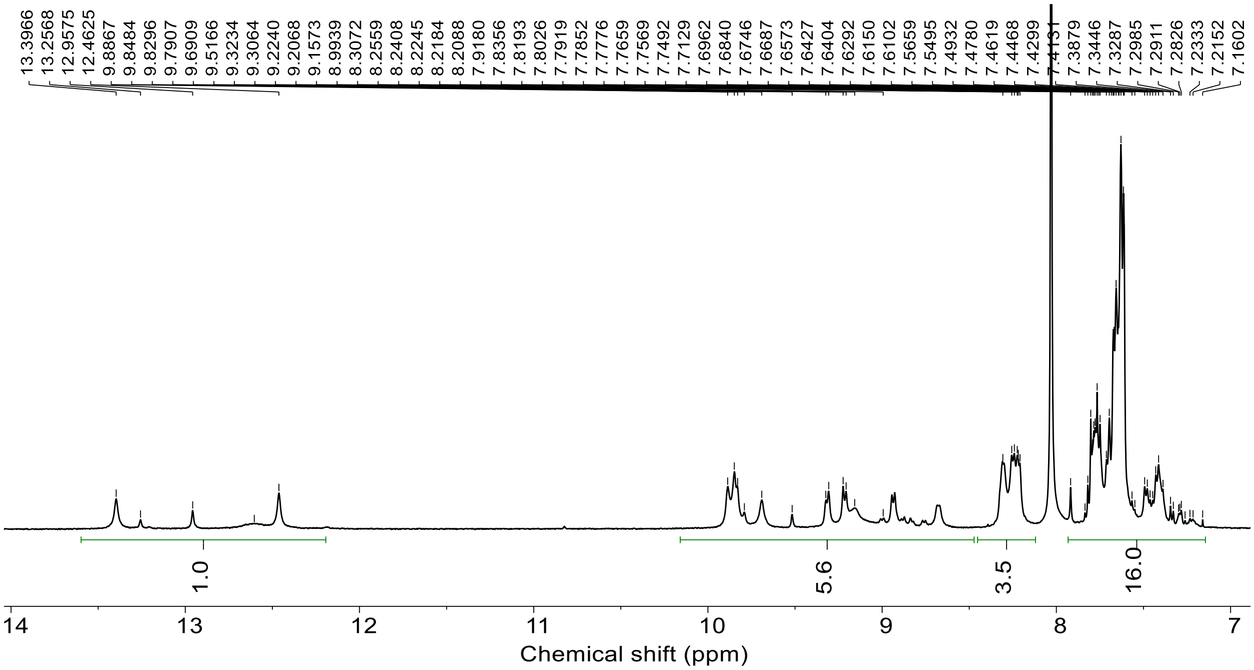

Figure S27. Aromatic region of ^{1}H NMR spectrum of a 1:1 solution of **4** and Zn(NTf$_2$)$_2$ (500 MHz, DMF-*d*$_7$, 298 K).

4 (4.2 mg, 0.0033 mmol, 1 equivalent) and Zn(NTf$_2$)$_2$ (10.3 mg, 0.016 mmol, 5 equivalent) were dissolved in DMF-*d*$_7$ at room temperature to obtain a yellow solution. A ^{1}H NMR spectrum was recorded.

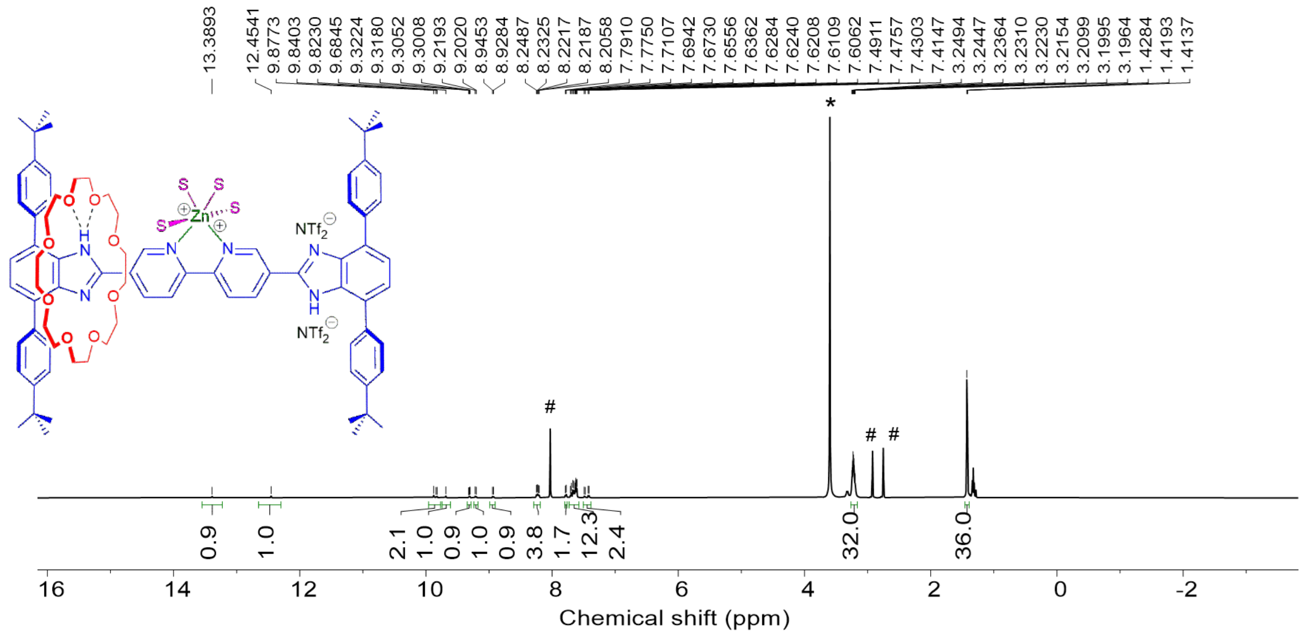

Figure S28. ^{1}H NMR spectrum of [Zn(DMF)$_4$(**4**)][NTf$_2$]$_2$ produced from a 1:5 equiv. solution of **4** and Zn(NTf$_2$)$_2$ (500 MHz, DMF-*d*$_7$, 298 K). # = residual DMF, * = water, *S* = solvent.

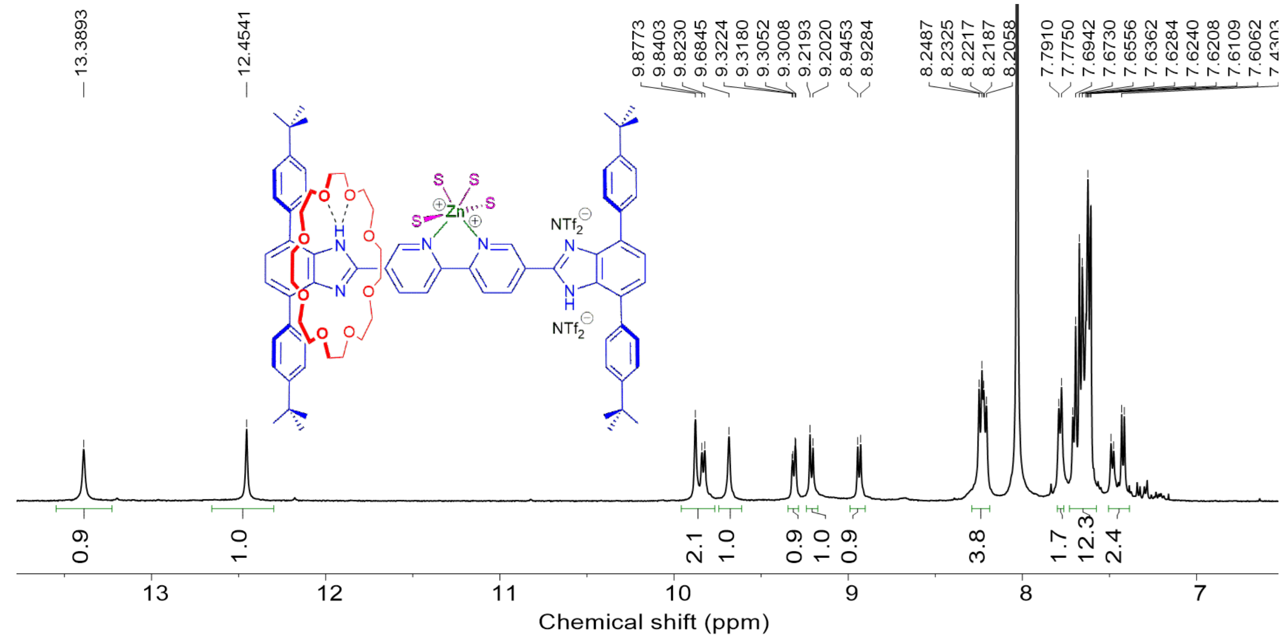

Figure S29. Aromatic region of the ^{1}H NMR spectrum of [Zn(DMF)$_4$(**4**)][NTf$_2$]$_2$ produced from a 1:5 equiv. solution of **4** and Zn(NTf$_2$)$_2$ (500 MHz, DMF-*d*$_7$, 298 K). *S* = solvent.

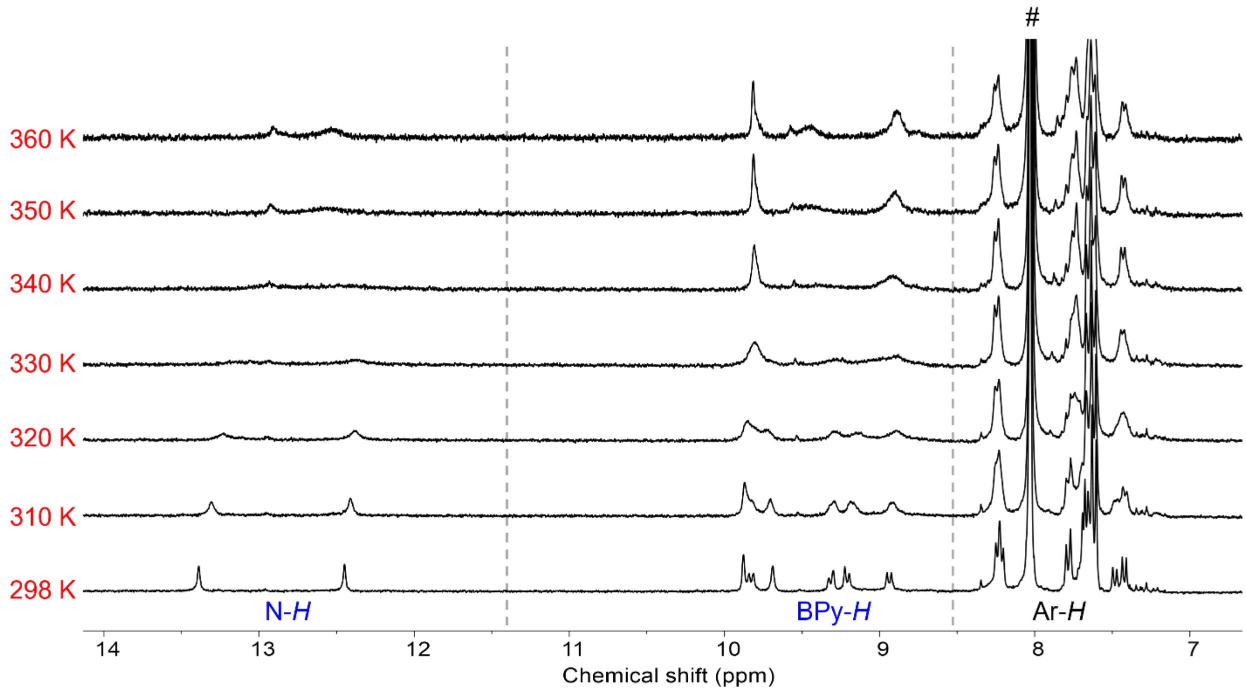

Figure S30. Aromatic region of the VT ^{1}H NMR spectra of $[Zn(DMF)_4(\mathbf{4})][NTf_2]_2$ produced from a 1:5 equiv. solution of **4** and $Zn(NTf_2)_2$ (500 MHz, DMF-d_7, 298 K).

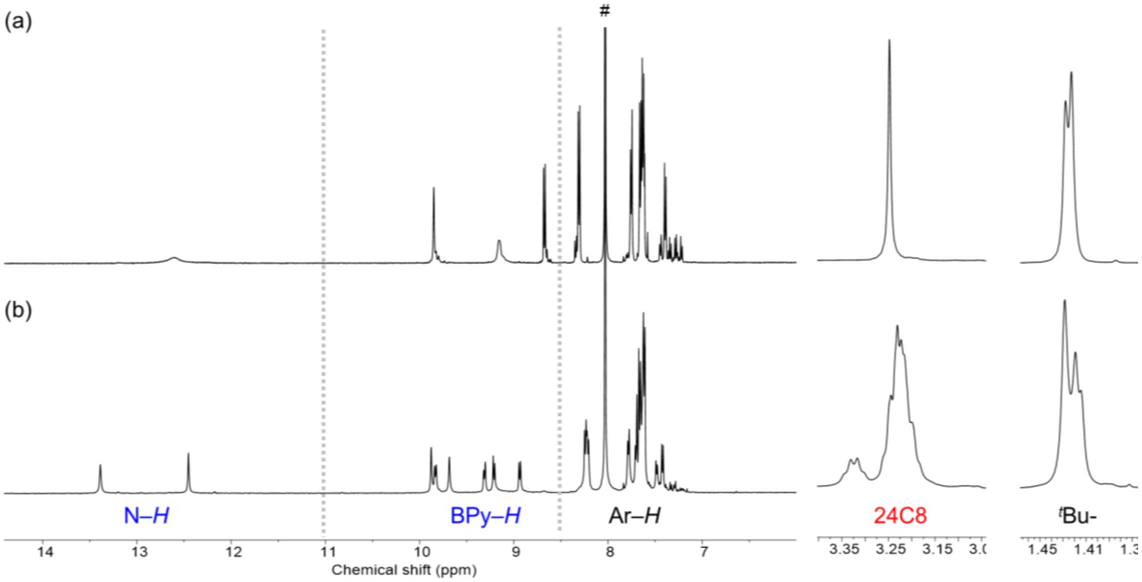

Figure S31. A comparison of the key regions of the ^{1}H NMR spectra of (a) **4** and (b) a solution of $[Zn(DMF)_4(\mathbf{4})][NTf_2]_2$ prepared by dissolving **4** and $Zn(NTf_2)_2$ in 1:5 equiv. ratio. (500 MHz, DMF-d_7, 298 K).

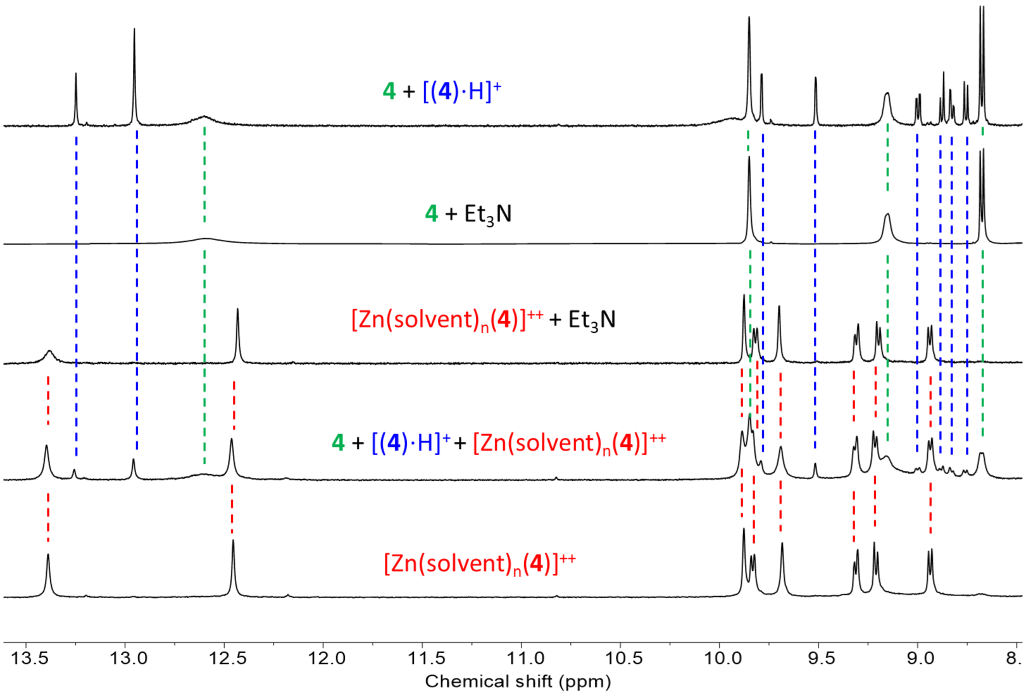

Figure S32. Partial ^{1}H NMR spectra, top to bottom: a solution of **4** and [H-**4**]$^+$, solution-a after the addition of Et_3N, solution-b after the addition of five equivalents of $Zn(NTf_2)_2$, a solution containing **4** and $Zn(NTf_2)_2$, in a 1:1 ratio, a solution containing **4** and $Zn(NTf_2)_2$, in a 1:5 ratio. (500 MHz, DMF-d_7, 298 K)

12. 2D EXSY of $[Zn(DMF)_4(4)][NTf_2]_2$ in DMF

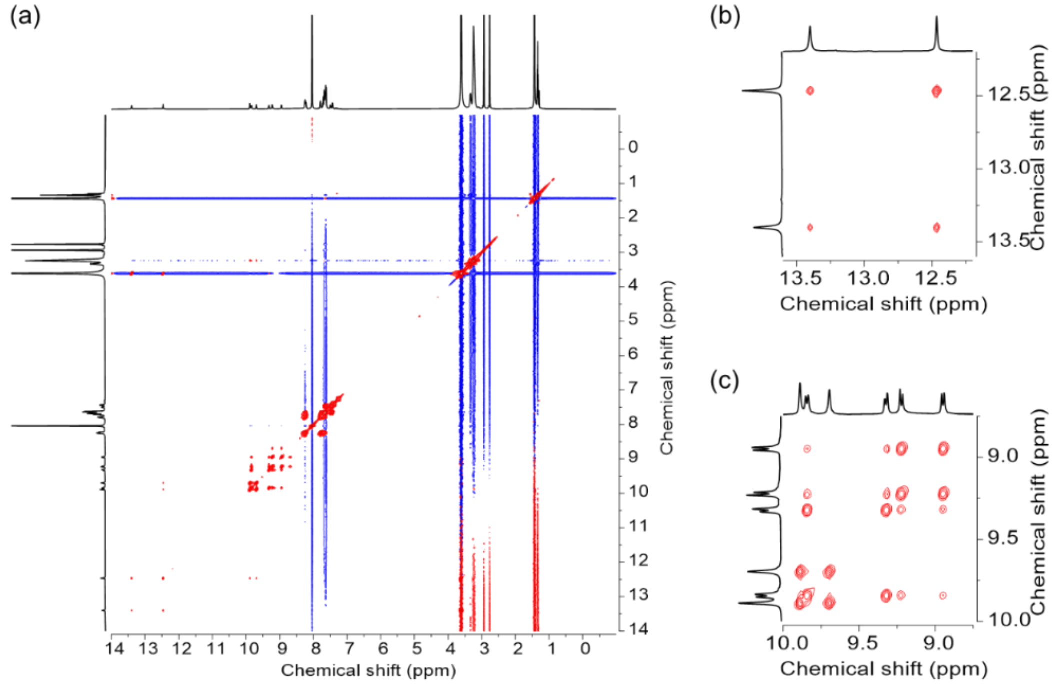

Figure S33. 2D EXSY ^{1}H-^{1}H NMR spectrum of $[Zn(DMF)_4(\mathbf{4})][NTf_2]_2$. Mixing time = 800 ms (a) Full spectrum, (b) N-*H* region, and (c) bipyridine (*BPy*) region. (500 MHz, DMF-d_7, 298 K) Based on integrations of the N-*H* cross-peaks, we determined the shuttling rate using the following calculations.[S3]

$$r = \frac{I_{AA}+I_{BB}}{I_{AB}+I_{BA}}$$

$$k = \frac{1}{\tau_m}\ln\frac{r+1}{r-1}$$

$$k = k_1 + k_{-1}$$

$$k_{obs} = k_1 = k_{-1}$$

$$\Delta G^{\ddagger} = -RT\ln\left(\frac{kh}{k_B T}\right)$$

$$R = 1.987\ \mathrm{cal{\cdot}K^{-1}{\cdot}mol^{-1}}$$

$$k_B = 3.30{\times}10^{-24}\ \mathrm{cal{\cdot}K^{-1}}$$

$$h = 1.58{\times}10^{-34}\ \mathrm{cal{\cdot}s}$$

$$\tau_m = 0.8\ \mathrm{s}$$

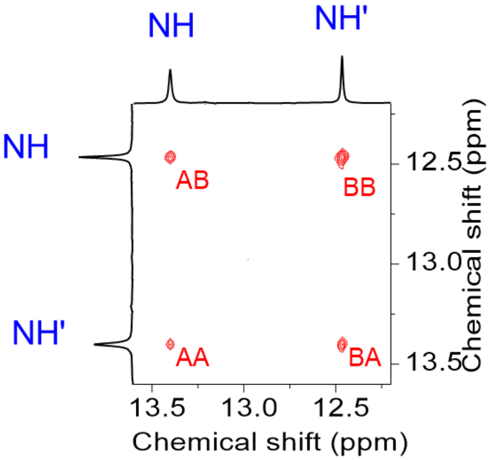

13. 2D ROESY of $[Zn(DMF)_4(\mathbf{4})][NTf_2]_2$ in DMF

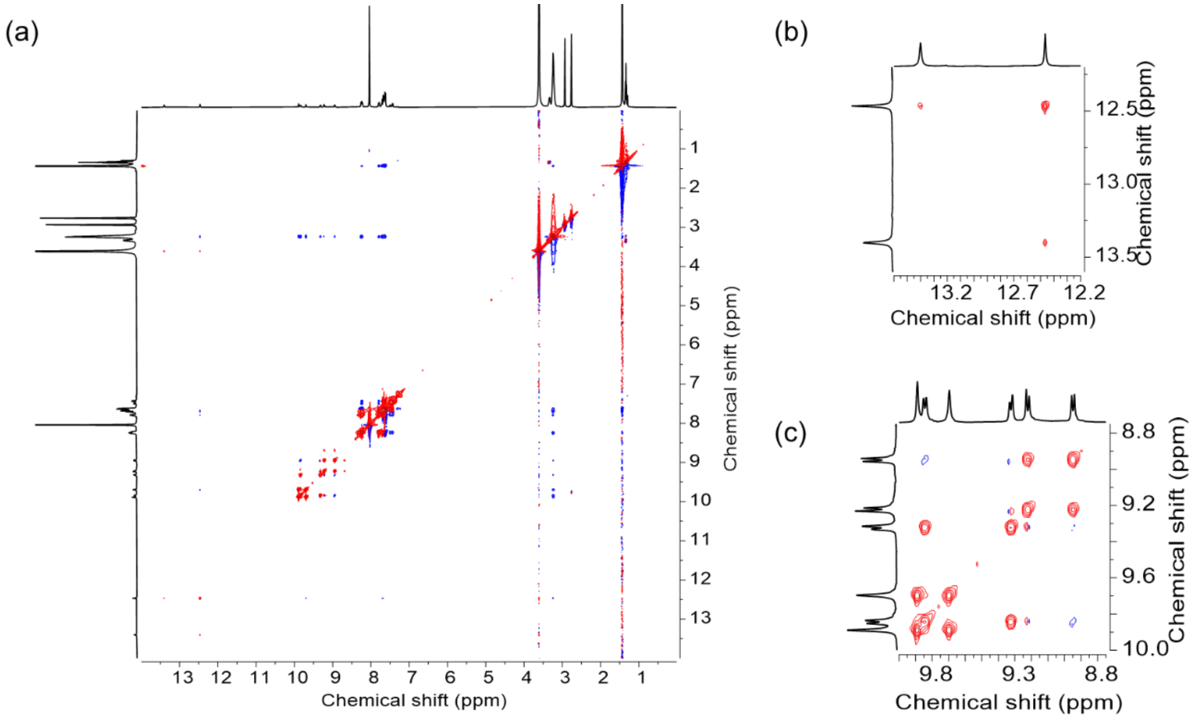

Figure S34. 2D ROESY ^1H-^1H NMR spectrum of $[Zn(DMF)_4(\mathbf{4})][NTf_2]_2$. (a) Full spectrum, (b) N-*H* region, and (c) bipyridine (*Bpy*) region. (500 MHz, DMF-d_7, 298 K). The main reason for collecting a 2D ROESY was to confirm whether the cross-peaks between the N-*H*s were due to exchange and because of through space coupling. The same phase for the cross-peaks and the diagonal peaks confirms that these are indeed exchange peaks between N-*H*s.

14. Single Crystal X-ray Diffraction Studies

General: Suitable single crystals were mounted on a glass micro-loop covered with perfluoro ether oil (Paratone® N). Crystallographic data were collected on Bruker D8 Venture diffractometer equipped with an Oxford Cryosystems low-temperature device operating at 170.0(1) K. Generic ϕ and ω scans (MoKα, λ = 0.71073 Å) were used for the data measurement. The diffraction patterns were indexed, and the unit cells refined with SAINT (Bruker, V.8.34A, after 2013) software. Data reduction, scaling and absorption correction were performed with SAINT and SADABS software (Bruker, 8.34A after 2013). [S4] A multi-scan absorption correction was applied within SADABS-2014/4 (Bruker, 2014/4). [S4] Space group determination was based upon analysis of systematic absences, E statistics, and successful refinement of all structures. The structures were solved by ShelXT (Sheldrick, 2015) structure solution program with Intrinsic phasing algorithm and refined with Least squares method by minimization of $\Sigma w(F_0^2 - F_c^2)^2$.[S5] SHELXL weighting scheme was used under 2018/3 version of ShelXL (Sheldrick, 2015).[S6] Structure solution, refinement and CIF compilation was performed within Olex2SyS software (Dolomanov, 2009).[S7] All non-hydrogen atoms were refined anisotropically. The positions of the hydrogen atoms were calculated geometrically and refined using the riding model. Neutral atom scattering factors for all atoms were taken from the International Tables for Crystallography. All of the crystallographic data were deposited in the Cambridge structural database. Graphic depiction of the X-ray structure were generated using CrystalMaker software.[S8]

Structure of 4: Single crystals were grown by vapour diffusion of diethyl ether into a saturated solution of **4** in toluene after four days. H2 atom residing on N2 was unequivocally located via analysis of Fourier difference maps, while the occupancy of H5 and H6 residing on N5 and N6 correspondingly were set to 0.5. 400 electrons were located in 1436 Å^3 voids that could be attributed to the mixture of toluene and diisopropyl ether co-crystallized. The diffuse nature of the electron density in the voids prevented modelling of the solvent molecules, and they were therefore masked using Olex2.mask algorithms. O2, O3, C69, C70, C71, C72, C80 atoms of crown ether were found to be disordered and split accordingly over two positions. SADI restraints were applied to maintain the bond distances within O-C-O links. EADP constraints were applied to the corresponding atoms split in two halves (e.g., O2-O2B; C70-C70B), which is condoned for severely disordered fragments since two positions represent the same atom.

Structure of [Zn(4)$_2$(DMF)(H$_2$O)][NTf$_2$]$_2$: Single crystals of the Zn-complex were grown by vapour diffusion of isopropyl ether into a saturated solution of a 1:1 mixture of ligand **4** and Zn(NTf$_2$)$_2$ in DMF after one month. Limited angular resolution attained for this dataset (≈1.0 Å) prevented convergence of the refinement due to oscillation of XYZ coordinates for the terminal tert-butyl groups. Triflimide anions were observed in the voids but were not modelled due to diffuse electron density in the voids caused by poor intensity of diffraction spots at high 2Theta angles. 332 electrons were located in 2624 Å^3 voids that could be attributed to the presence of two triflimide anions and co-crystallized solvents used for crystallization. Diffuse nature of the electron density in the voids prevented modelling of their contents and, therefore, they were masked using Olex2.mask algorithms. Disorder was modelled for C127 (C1F) and C128 (C1E) atoms. SADI restraints were applied to maintain the bond distances within O-C-O links. EADP constraints were applied to the corresponding atoms split in two halves (e.g., C127-C1F; C128-C1E), which is condoned for severely disordered fragments since two positions represent the same atom.

Table S1. Single Crystal X-ray Diffraction Data for **4** and $[Zn(\mathbf{4})_2(DMF)(H_2O)][NTf_2]_2$.

Compound	**4**	$[Zn(\mathbf{4})_2(DMF)(H_2O)][NTf_2]_2$
CCDC Number	2248267	2248268
Empirical formula	$C_{80}H_{96}N_6O_8$	$C_{163}H_{201}N_{13}O_{18}Zn$
Formula weight	1269.62	2695.73
Temperature/K	170.0(1)	170.0(1)
Crystal system	triclinic	triclinic
Space group	P-1	P-1
a/Å	14.9954(6)	19.9646(12)
b/Å	16.1533(7)	21.9566(14)
c/Å	20.1627(9)	22.5133(15)
α/°	86.179(2)	69.998(2)
β/°	74.935(2)	78.914(2)
γ/°	80.127(2)	81.231(2)
Volume/Å^3	4645.0(3)	9060.2(10)
Z	2	2
ρ_{calc}g/cm^3	0.908	0.988
μ/mm^{-1}	0.058	0.192
F(000)	1364	2888
Crystal size/mm^3	0.26 × 0.12 × 0.12	0.12 × 012 × 0.10
Radiation	MoKα (λ = 0.71073)	MoKα (λ = 0.71073)
2Θ range data collection/°	3.668 to 55.754	3.758 to 50.054
Index ranges	$-19 \le h \le 19$, $-21 \le k \le 21$, $-26 \le l \le 26$	$-23 \le h \le 23$, $-26 \le k \le 26$, $-26 \le l \le 26$
Reflections collected	254110	368177
Independent reflections	22158, R_{int} = 0.0663, R_{sigma} = 0.0331	31970, R_{int} = 0.1240, R_{sigma} = 0.0.0689
Data/restraints/parameters	22158/872/884	31970/225/1766
Goodness-of-fit on F^2	1.063	1.197
Final R indexes [I>=2σ (I)]	R_1 = 0.1078, wR_2 = 0.2715	R_1 = 0.1115, wR_2 = 0.3123
Final R indexes [all data]	R_1 = 0.1232, wR_2 = 0.2815	R_1 = 0.1795, wR_2 = 0.3687
Largest diff. peak/hole / e Å^{-3}	0.75/-0.59	1.13/-0.68

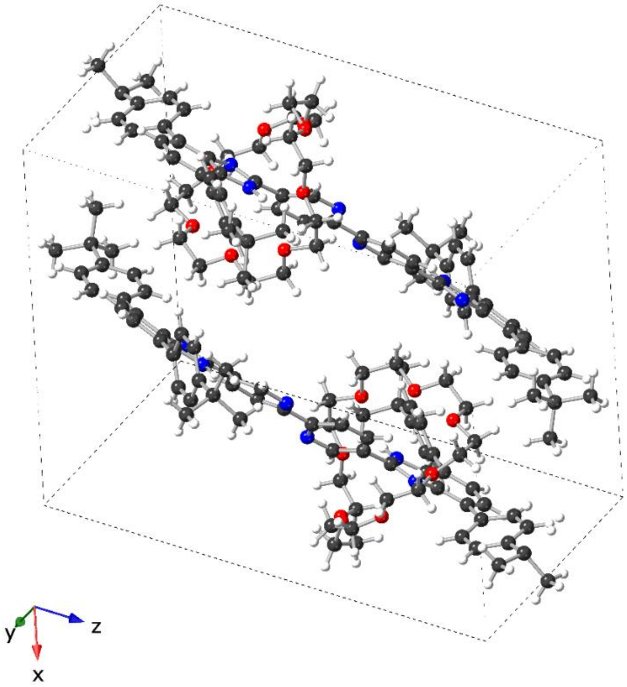

Figure S35. Molecular unit cell for crystal structure of rotaxane ligand **4**

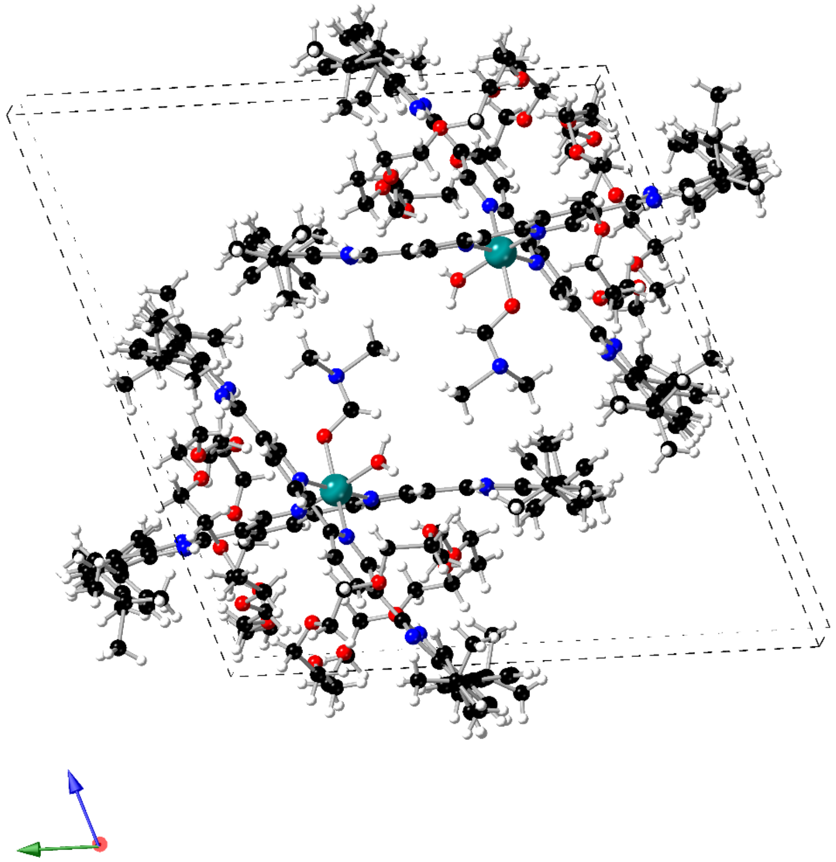

Figure S36. Molecular unit cell for crystal structure of complex [Zn(**4**)$_2$(DMF)(H$_2$O)][NTf$_2$]$_2$.

15. DFT Calculated Structure

DFT calculations were done using the program Jaguar.[S9] For the geometry optimization and vibrational frequency calculations of [Zn(**4**)(DMF)][NTf$_2$]$_2$, we used the B3LYP-D3/STO-3G* basis set without any constraints. There were no imaginary frequencies indicating the structure optimized was an energy minimum. Implicit solvation effects were incorporated using the Polarized Continuum Model (PCM) for dimethylformamide (DMF).

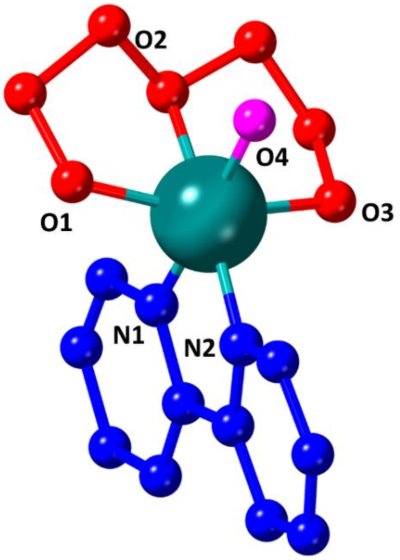

N1-Zn-N2 = 81.3°
N1-Zn-O1 = 96.1°
N1-Zn-O2 = 90.4°
N1-Zn-O3 = 85.8°
N1-Zn-O4 = 177.2°

N2-Zn-O1 = 101.9°
N2-Zn-O2 = 171.7°
N2-Zn-O3 = 97.9°
N2-Zn-O4 = 101.3°

O1-Zn-O2 = 79.2°
O1-Zn-O3 = 160.2°
O1-Zn-O4 = 82.2°

O2-Zn-O3 = 81.1°
O2-Zn-O4 = 87.1°

O3-Zn-O4 = 95.1°

Figure S37. The coordination sphere of the calculated octahedral complex listing the angles between donor atoms bound to Zn.

Atomic Coordinates for [Zn(4)(DMF)][NTf$_2$]$_2$

Zn1	12.6346974379	17.7360833738	5.7541763430
N2	13.9995406494	19.0990358266	5.3803813804
N3	14.1511720880	16.4484784847	5.7639646120
N4	14.0583140873	12.1589384176	5.9256062508
N5	16.3754546386	11.9763257918	5.9940311040
H6	17.3778379880	12.2566777055	6.0723120998
N7	13.4894099530	23.3866512613	4.4158497066
H8	12.5524363466	22.9856575002	4.6442881986
N9	15.7996992765	23.5674623628	4.2203127814
C10	15.2960477998	18.6052305098	5.5645937842
C11	16.4272188985	19.4542580894	5.4589511178
H12	17.4460299043	19.0411945259	5.6603069869
C13	16.2294480772	20.8036103723	5.1307098128
H14	17.0844612981	21.4895706715	5.0310254089
C15	14.9183779124	21.3183721149	4.9123380706
C16	13.8226363010	20.4297263865	5.0643804661
H17	12.7744174241	20.7410488763	4.9318614146
C18	14.7465424346	22.7431255573	4.5270075068

C19	13.7375373165	24.7163613895	4.0128851258
C20	15.1656875373	24.8193526783	3.9011346917
C21	15.7761572932	26.0673102861	3.5169354467
C22	14.8831245742	27.1427519458	3.3078354122
H23	15.2860084569	28.1262478444	3.0367301284
C24	13.4742318477	27.0190089616	3.4373047465
H25	12.8485803700	27.9017474754	3.2478142380
C26	12.8445327276	25.8042726053	3.7798073125
C27	11.3490993686	25.6631467002	3.8942795775
C28	10.5656647377	26.6964452280	4.4640455195
H29	11.0586454056	27.6040377425	4.8379700902
C30	9.1678963320	26.5696151907	4.5753888580
H31	8.6031283304	27.3911214417	5.0309776062
C32	8.4961154369	25.4104937033	4.1186952114
C33	9.2839379859	24.3823239608	3.5382310788
H34	8.7979983207	23.4728662741	3.1614999557
C35	10.6784851951	24.5007621380	3.4276774475
H36	11.2508334652	23.6964105297	2.9470077856
C37	6.9451471635	25.2282718170	4.2241179910
C38	6.6316107215	23.9421856309	5.0702339338
H39	7.0436209746	24.0430458338	6.0862234290
H40	7.0658101528	23.0470604811	4.6015159452
H41	5.5422101922	23.8022395081	5.1459090744
C42	6.2500327560	26.4526142621	4.9082144786
H43	5.1651921257	26.2729306024	4.9571042803
H44	6.4218217356	27.3749256864	4.3334565763
H45	6.6245569036	26.5961315333	5.9330729976
C46	6.3476671606	25.0586408791	2.7806628350
H47	6.7798832150	24.1813699101	2.2773853478
H48	6.5574552706	25.9516918813	2.1719234973
H49	5.2565985797	24.9236209548	2.8416034975
C50	17.2672533030	26.2241699582	3.3613643214
C51	17.8288176689	27.3021748144	2.6226056876
H52	17.1730174832	28.0345779942	2.1336594956
C53	19.2185787816	27.4376356679	2.4879202241
H54	19.6126552769	28.2788678006	1.9034936316
C55	20.1186424957	26.5126194684	3.0806431118
C56	19.5589487617	25.4389615412	3.8119426378
H57	20.2105206737	24.6948968434	4.2855999062
C58	18.1664648768	25.2954284391	3.9488808405
H59	17.7469144772	24.4411060664	4.4974037839
C60	21.6605594073	26.7052786433	2.8955805950
C61	22.0793948067	28.1091224433	3.4626557834
H62	21.5523743012	28.9187385293	2.9361643709
H63	23.1631768092	28.2554272362	3.3331974199
H64	21.8420982672	28.1751621704	4.5360721006
C65	22.0052408376	26.6388183064	1.3635387366
H66	21.7192612462	25.6599706443	0.9488768352

H67	23.0877659169	26.7792934825	1.2175754967
H68	21.4721253956	27.4246762770	0.8075296886
C69	22.4893543885	25.6034993321	3.6383675029
H70	22.2921651547	25.6252024570	4.7210054342
H71	23.5629572038	25.7864016230	3.4783567654
H72	22.2489700935	24.6017808903	3.2521101765
C73	15.3789388289	17.1232445065	5.8022363145
C74	16.6007998304	16.4333607123	6.0084173392
H75	17.5474665275	17.0262143482	6.1186967064
C76	16.5817747242	15.0283587126	6.0716082014
H77	17.5262645140	14.4850879542	6.2168965753
C78	15.3554243932	14.3178917313	5.9472876443
C79	14.1553938405	15.0727691644	5.8292104706
H80	13.1747952763	14.5722609230	5.7806630950
C81	15.2508898652	12.8364640789	5.9631840764
C82	15.8874939787	10.6520151760	5.9796917882
C83	14.4567663157	10.7759889099	5.9459830036
C84	13.6263301485	9.5982695118	5.9455537158
C85	14.3159974897	8.3659862881	6.0031580798
H86	13.7401653957	7.4326851952	6.0280285662
C87	15.7317052917	8.2697300277	6.0395186553
H88	16.1902490047	7.2722321888	6.0713413034
C89	16.5734132684	9.4015268145	6.0170410753
C90	18.0760414131	9.2972033275	6.0277271733
C91	18.8811971634	10.1610379251	5.2440002539
H92	18.4070101013	10.9109150862	4.5971587325
C93	20.2842395697	10.0484961226	5.2487609435
H94	20.8650865763	10.7344580337	4.6213303742
C95	20.9397050218	9.0716654827	6.0341273537
C96	20.1286017417	8.2041040994	6.8124758809
H97	20.6009070150	7.4331045837	7.4348676025
C98	18.7291699265	8.3091737919	6.8103883427
H99	18.1309979741	7.6281467245	7.4308320098
C100	22.4960767069	8.9137067516	6.0706665007
C101	22.8795472575	7.4711422869	5.5812501342
H102	23.9733630321	7.3478777069	5.6049464715
H103	22.5303320001	7.3119030604	4.5493082648
H104	22.4278913337	6.7043192289	6.2276550610
C105	23.0008554769	9.1147806894	7.5448232690
H106	22.5503017469	8.3717073148	8.2191310678
H107	22.7388470101	10.1214118949	7.9050715392
H108	24.0954095862	9.0020363804	7.5827239817
C109	23.2188728911	9.9561219988	5.1534748313
H110	22.9954198374	10.9845961067	5.4740401772
H111	22.9138101461	9.8356146619	4.1031137589
H112	24.3068559130	9.8024408574	5.2174265887
C113	12.1215059428	9.6675309695	5.9046650249
C114	11.3380498988	8.5522668612	5.5090758210

H115	11.8274782211	7.6202200508	5.1963856507
C116	9.9329525312	8.6191121036	5.4899550121
H117	9.3741524865	7.7318588699	5.1717838087
C118	9.2453512093	9.7989202897	5.8638101777
C119	10.0299615584	10.9161187203	6.2513098279
H120	9.5341315342	11.8517886908	6.5433343882
C121	11.4310556359	10.8570005675	6.2710952793
H122	12.0234871004	11.7388804877	6.5495556492
C123	7.6848421348	9.9137554717	5.8610854800
C124	6.9943505177	8.5834308868	5.4105201449
C125	7.2502604958	11.0576643756	4.8747951321
H126	7.6817273177	12.0226283670	5.1778902853
H127	6.1533527828	11.1522354568	4.8719814210
C128	7.1915195720	10.2636581366	7.3116444660
H129	6.0936975108	10.3486287619	7.3223574782
H130	7.6175125482	11.2186607676	7.6520606610
H131	7.4906191901	9.4732937876	8.0179273376
H132	7.5855008130	10.8278589253	3.8514070565
H133	5.9020328859	8.7178458750	5.4295646532
H134	7.2919671496	8.3113002208	4.3864513854
H135	7.2540121777	7.7559245985	6.0882834555
C135	19.3132636218	18.2730283320	7.5844363474
C136	18.1515880326	18.8984765597	8.4412057889
O137	16.9465055310	18.0498486158	8.4652037756
O138	18.7957281815	18.1411191714	6.2058842404
C139	17.0623555952	17.1133861232	9.6015877947
C140	15.8760606350	16.1013907416	9.4866501402
O141	14.6307783060	16.8848192808	9.3653677966
C142	13.5602315685	15.9368912395	9.0141700944
C143	12.2899629404	16.7789243066	8.6674413746
O144	12.7046643731	17.9234967329	7.7802609067
C145	11.8870454659	19.1316185394	8.0769857871
C146	10.5090286106	18.9728601601	7.3677147273
O147	10.8803027558	18.6433734054	5.9652610393
C148	9.8312016836	17.8653810952	5.2591407301
C149	19.8763788203	17.7258457649	5.2869274107
C150	19.2907439100	17.8295222835	3.8418808564
O151	18.1014183627	16.9603085613	3.7962319341
C152	17.4548887709	17.1630381547	2.4898166739
C153	16.1575674861	16.2861863057	2.4517317870
O154	15.0315031817	17.0951576168	2.9662378990
C155	13.7955469098	16.3561533468	2.6487698171
C156	12.5859656790	17.3408325117	2.7804262027
O157	11.8093482570	17.0912911791	4.0423317123
C158	10.4402904024	17.6663384695	3.8476065466
H159	19.6161194050	17.2787807598	7.9824737880
H160	20.1971866680	18.9483190984	7.6079523102
H161	18.5430682401	19.1254119753	9.4568747234

H162	17.8510490186	19.8541139826	7.9625930395
H163	18.0163131256	16.5390645194	9.5859970783
H164	17.0077008530	17.6601304135	10.5711343512
H165	16.0347261361	15.4581488655	8.5936077571
H166	15.8653599129	15.4409209763	10.3850047369
H167	13.8384148536	15.3027302274	8.1461170032
H168	13.2957982328	15.2553789649	9.8572956845
H169	11.5311522868	16.1543873433	8.1503183323
H170	11.8509736258	17.2061576559	9.5908921736
H171	11.7705021729	19.2732125701	9.1706163528
H172	12.4468373814	19.9825713090	7.6385709585
H173	9.9136761962	18.1487268927	7.8146484280
H174	9.9234682062	19.9169481862	7.3772580403
H175	9.6542164052	16.8986323464	5.7794355428
H176	8.8907572243	18.4543718675	5.2055265240
H177	20.1933643605	16.6820769152	5.5088687434
H178	20.7593225804	18.3953922265	5.3835621429
H179	20.0689590167	17.5133783508	3.1081238904
H180	19.0306509883	18.8920712098	3.6291491015
H181	18.1292833086	16.8563794235	1.6564831228
H182	17.1761244768	18.2306838255	2.3272494022
H183	16.3151089583	15.3683721433	3.0648734997
H184	15.9668139433	15.9679149262	1.4021643802
H185	13.6359723098	15.4783149785	3.3162925333
H186	13.8109018014	15.9801523628	1.6012296602
H187	11.8851367276	17.1851935576	1.9355224039
H188	12.9418567292	18.3944011689	2.7749423813
H189	9.8346201002	16.9616428863	3.2385085260
H190	10.5144013171	18.6477280880	3.3323632636

16. References

S1. D. A. Leigh, R. G. Pritchard, A. J. Stephens, A Star of David Catenane. *Nat. Chem.* **2014**, *11*, 978-982.

S2. E. M. Johnson, R. Haiges, S. C. Marinescu, Covalent-Organic Frameworks Composed of Rhenium Bipyridine and Metal Porphyrins: Designing Heterobimetallic Frameworks with Two Distinct Metal Sites. *ACS Applied Materials & Interfaces* **2018**, *44*, 37919-37927.

S3. K. Zhu, V. N. Vukotic, N. Noujeim, S. J. Loeb, Bis(benzimidazolium) axles and crown ether wheels: a versatile templating pair for the formation of [2]rotaxane molecular shuttles. *Chem. Sci.* **2012**, *11*, 3265-3271.

S4. Bruker *SAINT+ and SADABS*, Bruker AXS Inc.: Madison, Wisconsin, USA, **2012**.

S5. G. Sheldrick, SHELXT - Integrated space-group and crystal-structure determination. *Acta Cryst. Sect. A.* 2015**, 71**, 3-8.

S6. G. Sheldrick, Crystal structure refinement with SHELXL. *Acta Cryst. Sect. C,* 2015**, 71**, 3-8.

S7. O. V. Dolomanov, L. J. Bourhis, R. J. Gildea, J. A. K. Howard and H. Puschmann, OLEX2: a complete structure solution, refinement, and analysis program. *J. Appl. Crystallogr.* 2009, **42**, 339-341.

S8. CrystalMaker® Software Ltd, Oxford, England (www.crystalmaker.com).

S9. Bochevarov, A. D.; Harder, E.; Hughes, T. F.; Greenwood, J. R.; Braden, D. A.; Philipp, D. M.; Rinaldo, D.; Halls, M. D.; Zhang, J.; Friesner, R. A. Jaguar: A high-performance quantum chemistry software program with strengths in life and materials sciences. *Int. J. Quantum Chem* **2013**, *18*, 2110-2142.